Geophys. J. R. astr. Soc. (1971) **25,** 157–206.

The Excitation of the Chandler Wobble by Earthquakes

F. A. Dahlen

(Received 1970 December 29)

Summary

Elastic dislocation theory has been extended to deal with point tangential displacement dislocations in a spherically symmetric, self-gravitating Earth model with a fluid core and with arbitrary radial variations in density and in the elastic velocities. This theory may be used to compute the changes in the products of inertia of a realistic Earth model caused by the displacement on a fault of arbitrary location and orientation. It is found that, in general, the changes are several times greater than similar computations for a spherical, homogeneous Earth model would seem to suggest. The results are used to examine the hypothesis that earthquakes are responsible for the excitation of the Chandler wobble. An empirical earthquake moment–magnitude relationship is used together with the theory to estimate the total excitation of the Chandler wobble by all observed large earthquakes since 1904. Unfortunately, the uncertainties in the estimation of the moments of past large earthquakes preclude a really definite conclusion, but it appears likely from the results that the cumulative effect of past earthquakes is sufficient to maintain the observed level of excitation of the Chandler wobble. The theoretical effects on the Earth's polar path of two large recent earthquakes, the 1960 Chilean earthquake and the 1964 Alaskan earthquake, may be computed using fault parameters determined from reliable field observations, and these are compared with the observed polar motion data.

1. Introduction

The equations governing the force-free motion of a rigid body were derived by Euler in 1758. On the basis of this theory, he suggested in 1765 that the Earth, since it has an equatorial bulge, might undergo a free nutation or free wobble of its axis of figure about its axis of instantaneous rotation, which would remain essentially fixed in space in the absence of external torques. The free period of this motion should be $A/(C-A)$ sidereal days, where C and A are the axial and equatorial moments of inertia of the Earth. If this were so, then an observer located on the Earth, and thus fixed with respect to the axis of figure, should be able to observe a periodic variation in the latitude of his observatory with a period of about 10 months.

Following Euler's original suggestion, astronomers for many years searched their observations for evidence of a 10-month free nutation. In 1891, Chandler showed that observations of the variation of latitude contained no 10-month component, but were rather characterized by an annual term plus another term with a period of about 14 months, 40 per cent longer than Euler's predictions. Only one year later, Newcomb (1892) showed that the Eulerian period of nutation of the Earth

would in fact be increased by virtue of its elastic yielding. Love (1909) and Larmor (1909) later provided an elegant quantitative formulation relating the increase in period caused by elastic yielding to the Love number k. There are still some difficulties and uncertainties even today in computing the dynamical effects of the Earth's fluid core (Jeffreys & Vicente 1957a, b) and oceans (Munk & MacDonald 1960) on the dynamical or frequency-dependent Love number, but basically the observed 14-month period of the Earth's Eulerian nutation is well understood. This 14 month free motion of the instantaneous pole of rotation about the Earth's axis of figure (as seen by an observer on Earth) is today called the Chandler wobble.

The cause of the annual component of the Earth's wobble is also fairly well understood. This is a forced motion of the pole, driven primarily by seasonal variations in the distribution of the mass of the atmosphere. The complete theory to investigate this effect was first derived by Jeffreys (1916), and his conclusions were completely confirmed by the more recent analysis by Munk & Hassan (1961) of much more complete meteorological data.

The cause of the annual wobble is known, and the observed 14-month period of the Eulerian free wobble has been adequately explained. There are, however, to this day two outstanding problems in the interpretation of the polar motion data. The statistical properties of the Chandler wobble component appear to be those of a damped harmonic oscillator excited at random (Munk & MacDonald 1960). The unanswered questions are: what is the source of the excitation, and what is the mechanism of damping or dissipation? The dissipation has at various times been ascribed to the Earth's fluid core, to tidal friction at the ocean bottom, or to elastic afterworking in the mantle. In a comprehensive review, Munk & MacDonald (1960) decided that almost no proposed energy sink can be really eliminated. Their final conclusion is (p. 173): 'The situation is appallingly uncertain'. One reason for this uncertainty is that the actual numerical value of the observed Q or the observed decay time τ of the Chandler wobble is itself highly uncertain. The various attempts that have been made to measure the Q of the Chandler wobble are summarized and discussed in Section 4 of this paper.

The excitation of the Chandler wobble was traditionally ascribed (Jeffreys 1940; Rudnick 1956; Munk & MacDonald 1960) to the irregular or non-seasonal motions of the Earth's atmosphere. Munk & Hassan (1961) conducted a complete analysis of all available meteorological data in order to test this hypothesis, and found that the spectral density of the atmospheric variation at the Chandler period was too low by one to two orders of magnitude to account for the observed level of the Chandler wobble. It appears that motions of the Earth's atmosphere, whereas they do give rise to an annual wobble, have little to do with exciting the free Chandler wobble.

The Earth's fluid core has also been suggested as a possible source of excitation. Because the lower mantle is electrically conducting, secular variation of the Earth's main magnetic field produces corresponding fluctuations in an electromagnetic torque acting between the core and mantle. Rochester & Smylie (1965) have computed the equatorial component of this core–mantle coupling torque which would be produced by the observed changes in the main magnetic field. They concluded that this torque was several orders of magnitude too low to significantly excite the Chandler wobble; but this conclusion has been questioned (Stacey 1969), because the computation involved several simplifying assumptions. There has also been a recent suggestion (Hide 1969) that the predominant coupling across the core–mantle boundary may not be electromagnetic in origin at all, but may rather be pressure coupling due to bumps on the core–mantle interface. It is perhaps safest to say that the hypothesis that coupling at the core–mantle boundary is responsible for the excitation of the Chandler wobble has not yet been completely eliminated.

A third suggested mechanism for the generation of the Chandler wobble and one which has received a great deal of attention recently (see, e.g. Mansinha *et al.* 1970)

is that seismic activity excites the Chandler wobble. When an earthquake or seismic event occurs within the Earth, it produces an associated redistribution of the Earth's mass, and this redistribution of mass will certainly affect the motion of the rotation pole. The hypothesis that earthquakes are responsible for the excitation of the Chandler wobble was put forth quite early (Cecchini 1928; Munk & MacDonald 1960), primarily, it seems, because there appears to have been a rather sudden increase in Chandler wobble activity around 1907, and the two preceding years were years of intense seismic activity. This hypothesis was traditionally ruled out (Munk & MacDonald 1960) because quantitative considerations, using a block fault model for the earthquake fault displacement field, seemed to indicate that even the largest earthquakes did not produce nearly large enough mass shifts to significantly excite the Chandler wobble. The view that a block model provided an adequate picture of the displacement field associated with an earthquake fault mechanism was laid to rest by the work of Chinnery (1961), Maruyama (1964), and Press (1965). These authors used elastic dislocation theory in a homogeneous half-space to compute the fall-off with distance of the displacements, strains, and tilts associated with the motion on a fault. Press (1965) showed that residual strains of order 10^{-8} observed on strainmeters located at teleseismic distances from the focus of the 1964 March 28 Alaskan earthquake could be explained in terms of elastic dislocation theory.

Mansinha & Smylie (1967) pointed out that the existence of extensive residual strain fields associated with earthquakes meant that the hypothesis that earthquakes maintain the Chandler wobble should be re-examined. The effect of an earthquake on the Chandler wobble arises through the change in the inertia tensor of the Earth produced by the redistribution of mass associated with the residual displacement field. Mansinha & Smylie (1967) utilized the theoretical results of Press (1965) for a homogeneous half space model in an attempt to decide if the changes in the inertia tensor associated with large earthquakes were sufficiently large to maintain the observed level of Chandler wobble excitation. Their results were at best inconclusive; it is now clear that a homogeneous half space is far too simple a model of the Earth for this particular application.

One year later Smylie & Mansinha (1968) put forth an elegant and much simpler method of testing the earthquake excitation hypothesis. Suppose that the only changes with time of the Earth's inertia tensor occur suddenly at the time of large earthquake events, and suppose further that the Earth is perfectly elastic (no dissipation). Then to an observer located on Earth, the path of motion of the instantaneous pole of rotation would appear to be a series of circular arcs, with breaks between the circular arcs occurring at the times of large earthquakes. Each successive circular arc will have as centre the new axis of figure of the Earth, after the redistribution of mass associated with the earthquake (see the mathematical development in Section 2). In fact, since the actual Earth's Chandler wobble has a finite Q, the successive paths between earthquakes will not be circular arcs but will rather spiral in slowly (the radius will be reduced by e^{-1} in τ years). Smylie & Mansinha (1968), by fitting circular arcs to the polar motion data of the Bureau International de l'Heure, found what appeared to be a significant correlation of large magnitude ($M \geqslant 7{\cdot}5$) earthquakes with breaks in the polar path.

Unfortunately, a rigorous re-examination of the polar motion data by Haubrich (1970) failed to uphold the correlation found by Smylie & Mansinha (1968). Haubrich showed quite clearly that the supposed correlation lacked robustness; that small changes in the analysis procedure produced large changes in the results. For example, if one varied the analysis procedure so as to find only the largest breaks in the data (those associated with the largest shifts in the axis of figure or equilibrium pole), then it appeared that these largest breaks were not at all associated with earthquakes. Another major difficulty with the analysis of Smylie & Mansinha (1968) was that the equilibrium pole shifts which were observed in the polar motion data were about ten

times too large in comparison to the observed Chandler power. Haubrich concluded that the polar motion data of the Bureau International de l'Heure probably contained too much noise to allow detection of the Chandler wobble excitation, regardless of the source mechanism. He also pointed out that if a weak, non-robust correlation does exist between earthquakes and polar motion data, it could very well be a correlation between the earthquakes and the noise in the polar motion data. The question of noise in the polar motion data as well as the general question of the validity of the analysis procedure of Smylie & Mansinha (1968) and Haubrich (1970) is discussed further in Section 4 of this paper.

If Haubrich's conclusions regarding the rather severe contamination by noise of the polar motion data are correct, then it is clear that some other method must be used to test the hypothesis that earthquakes excite the Chandler wobble. The only alternative method seems to be to examine the catalogue of past seismic events to determine if seismic activity has been sufficient to maintain the observed level of Chandler wobble excitation. In order to do this, it is necessary to be able to compute quantitatively the effect of an individual earthquake on the inertia tensor of the Earth. In their first study, Mansinha & Smylie (1967) attempted to test the earthquake hypothesis in this manner, but as has been pointed out, their use of a homogeneous half space model to compute theoretical earthquake mass redistributions was far too simple. A significant advance was made by Ben-Menahem & Israel (1970), who advanced an elasticity theory of dislocations for a spherical, homogeneous, non-gravitating Earth model. They utilized this theory to compute the change in the inertia tensor of the Earth caused by a few typical seismic events. Since these results did not appear particularly promising, they did not then make a serious attempt to deduce the total amount of Chandler wobble excitation produced by all past events in the seismic catalogue. Furthermore, the results presented in the present paper make it appear that even their model of the Earth may be too simple to provide a solution to this particular problem (see Section 4 for a comparison of the work done here with their work).

The purpose of this paper is to attempt to utilize the data in the seismic catalogue to provide a test of the hypothesis that earthquakes are responsible for the excitation of the Chandler wobble. It is first shown how static elastic dislocation theory may be extended to deal with earthquake fault dislocations in a spherically symmetric, self-gravitating Earth model with a fluid core and with arbitrary radial variations in density and in the elastic velocities. This theory is then used to compute the theoretical change in the inertia tensor of a realistic Earth model which would be produced by the displacement on a fault of arbitrary location and orientation. These results are then used together with an empirical earthquake moment-magnitude relation of Brune (1968) to estimate the total excitation of the Chandler wobble by all observed large earthquakes since 1904.

The organization of the paper is as follows. The next two sections are primarily an exposition of the mathematical tools which are needed in order to make the computation. Section 2 is a discussion of the dynamics of the Chandler wobble, and Section 3 is a discussion of elastic dislocation theory in an arbitrary spherically symmetric Earth model. In Section 4, this theory is applied to the particular cases of the 1960 Chilean and 1964 Alaskan earthquakes. Section 5 is then for the most part a discussion of the input data; i.e. the observed Chandler wobble parameters (Q, total power, etc.), the seismic catalogue, and the moment-magnitude relation. Section 6 summarizes the results and conclusions of the analysis.

2. Chandler wobble dynamics

The linearized equations of motion governing the dynamics of the Earth's wobble have been derived in an extremely clear fashion by Munk & MacDonald (1960), and

this development will follow theirs. Consider as a Cartesian reference frame the so-called 'geographic' (Munk & MacDonald 1960, p. 11) reference frame which is considered fixed in a prescribed way to the astronomical observatories. The $\hat{\mathbf{x}}_3$ axis is taken to be aligned near the mean pole of rotation of the Earth; the $\hat{\mathbf{x}}_1$ axis is taken through the Greenwich meridian, and the $\hat{\mathbf{x}}_2$ axis is taken through the meridian 90° to the east of Greenwich. The origin is placed at the centre of mass of the Earth. Let $m_1(t)$ and $m_2(t)$ denote the $\hat{\mathbf{x}}_1$ and $\hat{\mathbf{x}}_2$ components of the angular displacement of the Earth's instantaneous axis of rotation from the reference axis $\hat{\mathbf{x}}_3$. Let C and A be the mean axial and equatorial moments of inertia of the Earth. Now, any deformation of the elastic Earth, such as that produced by an earthquake, will produce changes in the inertia tensor of the Earth. Denote the variable components $C_{ij}(t)$ (with respect to the geographic reference axes) by

$$\left.\begin{aligned} C_{11}(t) &= A + c_{11}(t) \\ C_{22}(t) &= A + c_{22}(t) \\ C_{33}(t) &= C + c_{33}(t) \\ C_{ij}(t) &= c_{ij}(t), \qquad i \neq j. \end{aligned}\right\} \tag{1}$$

The changes $c_{ij}(t)$ in the components of the inertia tensor are presumed to be small compared to both A and C.

The linearized equations governing the motion of the Earth's instantaneous pole of rotation with respect to the prescribed geographic reference frame can be shown to be (Munk & MacDonald 1960)

$$\left.\begin{aligned} \dot{m}_1 + \omega_0 m_2 &= A^{-1}(\Omega c_{23} - \dot{c}_{13}) \\ \dot{m}_2 - \omega_0 m_1 &= A^{-1}(-\Omega c_{13} - \dot{c}_{23}) \end{aligned}\right\} \tag{2}$$

Here ω_0 is the observed angular frequency of oscillation of the free Chandler wobble (about $1{\cdot}69 \times 10^{-7}$ radians per second, corresponding to a period of about 14 months); Ω is the mean angular velocity of diurnal rotation of the Earth ($7{\cdot}292 \times 10^{-5}$ radians per second); and A is the mean equatorial moment of inertia ($8{\cdot}042 \times 10^{37}$ kg m^2) The dots in the equations (2) indicate differentiation with respect to time. It is convenient to write $m = m_1 + im_2$ and $c = c_{13} + ic_{23}$, in which case the equations (2) take the form

$$\dot{m} - i\omega_0 m = A^{-1}(-\dot{c} - i\Omega c). \tag{3}$$

Equation (3) allows one to determine the motion $m(t)$ of the Earth's instantaneous pole of rotation in response to small changes $c(t)$ of the Earth's inertia tensor. Other forcing terms not pertinent to this discussion have been omitted from the right-hand sides of equations (2) and (3). One can allow for the damping of the Chandler wobble by taking as the Chandler wobble angular frequency the complex number

$$\omega_0 \left(1 + \frac{i}{2Q}\right)$$

where Q is the quality factor of the Chandler wobble and is related to the decay time by

$$Q = \frac{\omega_0 \tau}{2}. \tag{4}$$

If there are no changes in the inertia tensor of the Earth, $c(t) = 0$, then the homogeneous solution to equation (3) merely represents the undisturbed free wobble. Suppose that the only changes in the inertia tensor of the Earth are those actually

produced by the earthquake events (see Section 4 for a comment on the validity of this assumption). Each earthquake event causes an associated redistribution of mass in the Earth which gives rise to a change with time $c(t)$ of the inertia tensor. In general, the redistribution of mass associated with an earthquake is completed in a time which is short compared to the Chandler wobble period, so that for the change $c(t)$ due to the jth earthquake one may write

$$\left.\begin{aligned} c(t) &= \Delta C_j H(t-t_j) \\ \dot{c}(t) &= \Delta C_j \delta(t-t_j) \end{aligned}\right\} \tag{5}$$

where $H(t)$ is the unit step function and t_j is the time of occurrence. For a single change $c(t)$ of the form (5) the solution to equation (3) takes the form

$$m(t) = m_0 \exp[i\omega_0(t-t_0)] + \left[\frac{\Omega}{\omega_0}\frac{\Delta C_j}{A} - \frac{(\Omega+\omega_0)}{\omega_0}\frac{\Delta C_j}{A}\exp[i\omega_0(t-t_j)]\right] H(t-t_j) \tag{6}$$

where $m(t_0) = m_0$ is the initial position of the pole. The polar motion produced by a sequence of N earthquakes is obtained by summing a series of solutions of the form (6)

$$m(t) = m_0 \exp[i\omega_0(t-t_0)] + \sum_j^N \left[\frac{\Omega}{\omega_0}\frac{\Delta C_j}{A} - \frac{(\Omega+\omega_0)}{\omega_0}\frac{\Delta C_j}{A}\exp[i\omega_0(t-t_j)]\right] H(t-t_j). \tag{7}$$

The motion of the rotation pole given in (7) can be easily visualized. Between earthquake events, the Earth's instantaneous pole of rotation wobbles freely about a mean pole of rotation which is identical with the axis of figure at that time. The redistribution of mass accompanying the earthquake at time t_j produces a sudden shift of the Earth's axis of figure to a new position, and at time t_j the instantaneous pole of rotation begins to wobble about the new axis of figure. For each earthquake events, the shift S_j of the mean pole of rotation (or, equivalently, the shift of the Earth's axis of figure) is given by

$$S_j = \frac{\Omega}{\omega_0}\frac{\Delta C_j}{A}. \tag{8}$$

If one can compute the changes ΔC_{13j} and ΔC_{23j} in the inertia tensor components of the elastic, self-gravitating Earth which are produced by any individual earthquake, then one can determine the pole shift S_j produced by that earthquake. Note that the approximation of $c(t)$ due to an earthquake source by a step function time dependence considerably simplifies the elastic-gravitational problem. It is only necessary to compute the net static displacement field produced by the earthquake in order to determine ΔC_{13j} and Δ_{23j}, the net change in the inertia tensor components. The dynamics of the elastic-gravitational displacement problem (i.e. the excitation of elastic-gravitational normal modes which decay in a time short compared to the Chandler wobble period) can be neglected.

Any attempt to deduce the theoretical total excitation of the Chandler wobble by a series of past earthquakes could of course be based on equation (7) (see Mansinha & Smylie 1967); it is, however, more convenient to consider the excitation process in the frequency domain. Going back to equation (3), denote the right-hand side of this equation by $\psi(t)$

$$\psi(t) = A^{-1}[-\dot{c}(t) - i\Omega c(t)]. \tag{9}$$

The time series $\psi(t)$ can be called the excitation function or the excitation process; knowledge of $\psi(t)$ allows a determination of the response $m(t)$ of the pole to the excitation process. For the case of the excitation by a series of N earthquake events, the excitation function takes the form

$$\psi(t) = \sum_j^N \left[-\frac{\Delta C_j}{A}\delta(t-t_j) - i\Omega\frac{\Delta C_j}{A}\delta(t-t_j) \right]. \tag{10}$$

It is easily shown that the terms $(\Delta C_j/A)\,\delta(t-t_j)$ are in fact small (by a factor ω_0/Ω) compared to the terms $(\Delta C_j/A)H(t-t_j)$; thus the excitation function for a series of of N earthquakes is essentially

$$\psi(t) = -i\Omega \sum_j^N \frac{\Delta C_j}{A} H(t-t_j). \tag{11}$$

The Chandler wobble excitation spectral density $S(\omega)$ is defined as the Fourier transform of the autocorrelation of the excitation process $\psi(t)$. The Fourier transform of a unit step function $H(t)$ is simply $(1/\omega)$ (except at $\omega = 0$). Utilizing this fact, it can be shown that the excitation spectral density resulting from a series of N earthquakes is

$$S(\omega) = \frac{1}{\omega^2}\langle R^2\rangle \tag{12}$$

where

$$\langle R^2\rangle = \frac{1}{T_N}\left|\sum_j^N S_j \exp(-i\omega_0 t_j)\right|^2 \tag{13}$$

is the mean square pole step per unit time interval produced by the earthquakes. Here T_N is the total time over which the earthquake summation is made. The total Chandler wobble power produced by the earthquake series is obtained by multiplying the excitation spectral density $S(\omega)$ by the resonance response of the Chandler wobble to any excitation process and then integrating over all frequencies. If the Q of the Chandler wobble is assumed to be fairly large, then the total Chandler wobble power P can be simply expressed in terms of the excitation spectral density at the Chandler wobble frequency ω_0 (Munk & Hassan 1961; Haubrich 1970).

$$P = \omega_0 QS(\omega_0) = \frac{Q}{\omega_0}\langle R^2\rangle. \tag{14}$$

The total Chandler wobble power produced by a series of earthquake occurrences is thus proportional to the Q of the Chandler wobble and proportional to the mean square pole shift per unit time produced by the earthquake sequence. To compute the total Chandler power produced by past earthquakes, one must be able to compute or estimate the sum (13) which defines the mean square angular displacement per unit time of the mean rotation pole. Excitation of the Chandler wobble by earthquakes may be thought of as a two-dimensional random walk process. The magnitude $|S_j|$ of each step in the walk is the net shift of the mean rotation pole produced by the jth earthquake and may be computed using (8). The direction of each step depends on the geometrical properties (location and orientation of the fault plane) of the earthquake, since S_j is complex, and also on the time t_j of the earthquake, because of the phase factor $\exp(-i\omega_0 t_j)$ in (13). The sum $\langle R^2\rangle$ is a measure of the mean square excursion per unit time from the origin of the random walk, or equivalently, the mean square pole shift per unit time.

The method of testing the earthquake hypothesis is thus to compute the total Chandler power produced by all past catalogued earthquakes and to compare to the observed Chandler power as measured from astronomical data. The computation involves two steps. The first step, discussed in Section 3, is to compute the mean pole shift

$$S_j = \left(\frac{\Omega}{\omega_0}\right) \frac{\Delta C_j}{A}$$

produced by an arbitrary earthquake. The second step, discussed in Section 5, is to estimate the sum $\langle R^2 \rangle$, the net effect of all past earthquakes, from the available data in the seismic catalogue.

3. Elastic dislocation theory

Consider a model of the Earth which consists of a self-gravitating elastic continuum occupying a volume V with exterior surface ∂V. It will be assumed that any earthquake occurring in the Earth can be modelled completely by specifying a jump discontinuity in displacement across a fault surface $\sum_0$ embedded somewhere in the Earth model V. It will be shown how elastic dislocation theory can be used to compute the associated static elastic-gravitational displacement field throughout V in terms of the prescribed fault slip on the earthquake fault surface $\sum_0$.

For the purpose of actually computing numerically the static elastic-gravitational displacement field associated with an earthquake, it is necessary to make certain simplifying assumptions in defining the Earth model V. While it is not really necessary to introduce these assumptions at this stage of the discussion, this will be done for convenience. It will first be assumed that the effect of the steady diurnal rotation of the Earth can be neglected in the Earth model V. It is further convenient to neglect in V the effect of any static non-isotropic stress field (such as that which acts to support surface topographic features) which may exist in the real Earth. It can be shown that the equilibrium shape of any such non-rotating, hydrostatic, self-gravitating configuration V is necessarily spherically symmetric. It will be further assumed that the dynamic stress–strain relation at every point in the Earth model is perfectly elastic, and furthermore is isotropic.

The Earth model V under consideration in this section is thus an arbitrary SNREI (spherical, non-rotating, elastic, isotropic) Earth model (Dahlen 1968). A SNREI Earth model of radius a can be completely characterized by three functions of r, the radial distance from the centre. These three functions are the density $\rho_0(r)$, the bulk modulus $\kappa(r)$, and the shear modulus $\mu(r)$, the latter two being the *in situ* elastic parameters appropriate to the hydrostatically compressed state of the material. Alternatively, one can describe a SNREI Earth model in terms of the three functions $\rho_0(r)$, $v_P(r)$, $v_S(r)$ where $v_P(r)$ and $v_S(r)$ are the *in situ* velocities of elastic compressional and shear waves; the relations between the elastic velocities and the elastic parameters are

$$\left.\begin{aligned} v_P^{\,2} &= \frac{\kappa + \frac{4}{3}\mu}{\rho_0} \\ v_S^{\,2} &= \frac{\mu}{\rho_0} \end{aligned}\right\} \tag{15}$$

Let $\phi_0(r)$ be the gravitational potential of the spherically symmetric Earth model V.

Then $\phi_0(r)$ may be computed in terms of the mass distribution $\rho_0(r)$ by utilizing the relation

$$\partial_r \phi_0(r) = 4\pi G r^{-2} \int_0^r dr\, r^2\, \rho_0(r). \tag{16}$$

Consider now a static body force $\mathbf{f}(\mathbf{r})$ applied to the Earth model V. Let $\mathbf{u}(\mathbf{r})$ be a static displacement field in response to this body force, and let $\phi_1(\mathbf{r})$ be the associated disturbance in the static gravitational potential. Then the equations relating $\mathbf{u}(\mathbf{r})$ and $\phi_1(\mathbf{r})$ to the applied body force $\mathbf{f}(\mathbf{r})$ are

$$\begin{aligned} -\rho_0 \nabla\phi_1 - \rho_1 \nabla\phi_0 - \nabla(\mathbf{u}.\rho_0 \nabla\phi_0) + \nabla.\mathbf{E} + \mathbf{f} &= \mathbf{0} \\ \nabla^2 \phi_1 &= 4\pi G \rho_1 . \end{aligned} \tag{17}$$

In the equations (17), the second order tensor $\mathbf{E}(\mathbf{r})$ is the (Lagrangian) elastic stress tensor associated with the elastic deformation $\mathbf{u}(\mathbf{r})$. At any point $\mathbf{r}$ in the body and to first order in the displacement field $\mathbf{u}$, $\mathbf{E}$ is related to $\mathbf{u}$ by the linear elastic parameters appropriate to the compressed state of the material at $\mathbf{r}$.

$$\mathbf{E} = (\kappa - \tfrac{2}{3}\mu)(\nabla.\mathbf{u})\,\mathbf{I} + \mu[\nabla\mathbf{u} + (\nabla\mathbf{u})^T] \tag{18}$$

where $\mathbf{I}$ is the second order identity tensor and $(\nabla\mathbf{u})^T$ is the transpose of $\nabla\mathbf{u}$. The quantity $\rho_1(\mathbf{r})$ is the change in density due to the displacement field $\mathbf{u}(\mathbf{r})$; $\rho_1(\mathbf{r})$ is related to $\mathbf{u}(\mathbf{r})$ through the linearized continuity equation

$$\rho_1 = -\nabla.(\rho_0\,\mathbf{u}). \tag{18'}$$

The equations (17) may also be written in terms of components defined with respect to the geographic reference axes $\hat{\mathbf{x}}_1$, $\hat{\mathbf{x}}_2$, $\hat{\mathbf{x}}_3$ which were introduced in Section 2.

$$\begin{aligned} -\rho_0 \partial_i \phi_1 + \partial_j(\rho_0 u_j)\partial_i\phi_0 - \partial_i(u_j \rho_0 \partial_j \phi_0) + \partial_j E_{ij} + f_i &= 0 \\ \partial_j \partial_j \phi_0 &= -4\pi G \partial_j(\rho_0 u_j). \end{aligned} \tag{19}$$

Consider as well a second applied body force $\mathbf{g}(\mathbf{r})$ which gives rise to a static displacement field $\mathbf{v}(\mathbf{r})$ with associated stress and gravitational perturbation fields $\mathbf{D}(\mathbf{r})$ and $\psi_1(\mathbf{r})$. Then

$$\begin{aligned} -\rho_0 \partial_i \psi_1 + \partial_j(\rho_0 v_j)\partial_i\phi_0 - \partial_i(v_j \rho_0 \partial_j \phi_0) + \partial_j D_{ij} + g_i &= 0 \\ \partial_j \partial_j \psi_1 &= -4\pi G \partial_j(\rho_0 v_j). \end{aligned} \tag{20}$$

Now take the dot product of $\mathbf{v}(\mathbf{r})$ with the first of the equations (19) and integrate the result over the volume V of the Earth model. Several applications of Gauss' theorem yield the relation

$$\mathscr{V}(\mathbf{u},\mathbf{v}) = \int_V dV\,[v_i f_i] - \int_{\partial V} dS n_j \left[v_i E_{ij} + \psi_1 \left(\frac{1}{4\pi G} \partial_j \phi_1 + \rho_0 u_j \right) \right]_-^+ . \tag{21}$$

Here $\mathscr{V}(\mathbf{u},\mathbf{v})$ is the potential energy bilinear form (Backus & Gilbert 1967; Dahlen 1968).

$$\begin{aligned} \mathscr{V}(\mathbf{u},\mathbf{v}) = \int_V dV\,[\kappa\,(\partial_i u_i)(\partial_j v_j) + \mu \Delta_{ij}\,\Gamma_{ij} + \rho_0 v_i u_j \partial_i \partial_j \phi_0 + \rho_0 \partial_j \phi_0 (v_i \partial_i u_j - v_j \partial_i u_i) \\ + \rho_0 v_i \partial_i \phi_1 + \rho_0 u_i \partial_i \psi_1] + \int_E dV \left(\frac{1}{4\pi G} \partial_j \phi_1 \partial_j \psi_1 \right). \end{aligned} \tag{22}$$

In (22), E is all of space and Δ_{ij} and Γ_{ij} are the Cartesian components of the strain

deviator tensors associated with the displacement fields $\mathbf{u}$ and $\mathbf{v}$. Therefore

$$\left.\begin{aligned}\Delta_{ij} &= \tfrac{1}{2}(\partial_i u_j + \partial_j u_i) - \tfrac{1}{3}(\partial_k u_k)\delta_{ij} \\ \Gamma_{ij} &= \tfrac{1}{2}(\partial_i v_j + \partial_j v_i) - \tfrac{1}{3}(\partial_k v_k)\delta_{ij}.\end{aligned}\right\} \tag{23}$$

In (21), $\hat{\mathbf{n}}$ is the unit outward normal of the surface ∂V, and for any vector field $\mathbf{f}$ defined in E, $[\mathbf{f}]^+$ is the jump discontinuity in $\mathbf{f}$ across ∂V. An expression similar to (21) may be derived by taking the dot product of $\mathbf{u}(\mathbf{r})$ with the first of the equations (20) and then integrating over V.

$$\mathscr{V}(\mathbf{v}, \mathbf{u}) = \int_V dV\,[u_i g_i] - \int_{\partial V} dS n_j \left[u_i D_{ij} + \phi_1 \left(\frac{1}{4\pi G}\,\partial_j \psi_1 + \rho_0 v_j\right)\right]^+_- . \tag{24}$$

Now the potential energy bilinear form is symmetric, i.e.

$$\mathscr{V}(\mathbf{u}, \mathbf{v}) = \mathscr{V}(\mathbf{v}, \mathbf{u}) \tag{25}$$

Therefore one can write $\int_V dV\,[\mathbf{v}.\mathbf{f}] - \int_{\partial V} dS n_j \left[v_i E_{ij} + \psi_1 \left(\frac{1}{4\pi G}\,\partial_j \phi_1 + \rho_0 u_j\right)\right]^+_-$

$$= \int_V dV\,[\mathbf{u}\cdot\mathbf{g}] - \int_{\partial V} dS n_j \left[u_i D_{ij} + \phi_1 \left(\frac{1}{4\pi G}\,\partial_j \psi_1 + \rho_0 v_j\right)\right]^+_- . \tag{26}$$

The relation (26) is simply an extension of the Betti reciprocal theorem (Love 1927) to the case of an elastic configuration which is self-gravitating. The Betti reciprocal theorem is a global relation between any two possible but different sets of solutions to the static gravitational-elastic equations (17). Although (26) has been derived here only for a SNREI Earth model V, it is possible to demonstrate its validity for an arbitrary non-SNREI Earth model. Now a specific application of this reciprocal relation will be made in order to deduce the fundamental relation of elastic dislocation theory. (Volterra 1907; Steketee 1958; Maruyama 1963, 1964).

First note that in (26), the volume V and surface ∂V of integration need not be the actual physical volume V and exterior surface ∂V of the Earth model; the derivation is unchanged if the volume of integration is any arbitrary volume V', as long as the surface of integration $\partial V'$ is the surface of V'. For this specific application, consider a volume of integration V' in (26) consisting of the volume V of the Earth minus a small interior volume element V_0. The surface integral in (26) is then taken over the exterior surface ∂V of the Earth model plus the surface ∂V_0 of the small interior volume element. The unit normal $\hat{\mathbf{n}}_0$ must of course be taken to be the unit inward normal of ∂V_0 (this is the unit outward normal of the integration volume). Later the volume V_0 of the interior volume element will be allowed to shrink to zero in such a manner that the surface area ∂V_0 does not shrink to zero; the resulting surface element ∂V_0 will be used to represent an earthquake fault surface Σ_0. The relation (26) now takes the form

$$\begin{aligned}\int_{V-V_0} dV\,[\mathbf{v}.\mathbf{f}] &- \int_{\partial V} dS n_j \left[v_i E_{ij} + \psi_1 \left(\frac{1}{4\pi G}\,\partial_j \phi_1 + \rho_0 u_j\right)\right]^+_- \\ &- \int_{\partial V_0} dS_0 n_j^0 \left[v_i E_{ij} + \psi_1 \left(\frac{1}{4\pi G}\,\partial_j \phi_1 + \rho_0 u_j\right)\right]^+_- \\ = \int_{V-V_0} dV\,[\mathbf{u}.\mathbf{g}] &- \int_{\partial V} dS n_j \left[u_i D_{ij} + \phi_1 \left(\frac{1}{4\pi G}\,\partial_j \psi_1 + \rho_0 v_j\right)\right]^+_- \\ &- \int_{\partial V_0} dS n_j^0 \left[u_i D_{ij} + \phi_1 \left(\frac{1}{4\pi G}\,\partial_j \psi_1 + \rho_0 v_j\right)\right]^+_- .\end{aligned} \tag{27}$$

Now in (27) take the body force $\mathbf{g}$ to be zero everywhere and take $\mathbf{f}$ to be a unit point force located at an arbitrary point $\mathbf{r}$ in the volume V and pointing in an arbitrary direction $\hat{\mathbf{x}}_k$. Take $\mathbf{u}$, $\mathbf{E}$, and ϕ_1 to represent the static elastic-gravitational response of the Earth model V to the unit point force $\mathbf{f}$; then $\mathbf{u}$, $\mathbf{E}$, and ϕ_1 are the unique solutions in V to the static equations (17) which satisfy the physical boundary conditions on ∂V (Alterman, Jarosch & Pekeris 1959; Backus 1967)

$$\left.\begin{aligned} &\hat{\mathbf{n}}\cdot\mathbf{E} = \mathbf{0} \\ &\hat{\mathbf{n}}\cdot\left[\frac{1}{4\pi G}\nabla\phi_1 + \rho_0\,\mathbf{u}\right]_-^+ = 0. \end{aligned}\right\} \tag{28}$$

The existence of the imaginary interior volume element V_0 is not taken into account in the computation of $\mathbf{u}$, $\mathbf{E}$, and ϕ_1; i.e. the quantities

$$\mathbf{u}, \phi_1, \hat{\mathbf{n}}_0\cdot\mathbf{E}, \hat{\mathbf{n}}_0\cdot\left[\frac{1}{4\pi G}\nabla\phi_1 + \rho_0\,\mathbf{u}\right]$$

are continuous across ∂V_0 (as well as everywhere else within V except at any solid-liquid discontinuity within V, where only $\hat{\mathbf{n}}.\mathbf{u}$ and not $\mathbf{u}$ need be continuous). Take $\mathbf{v}$, $\mathbf{D}$, and ψ_1 to represent solutions to the equations (20) with the applied body force $\mathbf{g}$ equal to zero everywhere; the static elastic-gravitational fields $\mathbf{v}$, $\mathbf{D}$, and ψ_1 are considered to be produced in V not by an applied body force but by the action of various prescribed boundary conditions on the interior surface element ∂V_0. On the exterior surface ∂V, the usual boundary conditions are satisfied

$$\left.\begin{aligned} &\hat{\mathbf{n}}\cdot\mathbf{D} = \mathbf{o} \\ &\hat{\mathbf{n}}\cdot\left[\frac{1}{4\pi G}\nabla\psi_1 + \rho_0\,\mathbf{v}\right]_-^+ = 0. \end{aligned}\right\} \tag{29}$$

Now consider the form of the various terms in the Betti reciprocal relation (27). The volume integral containing the body force $\mathbf{g}$ has the value zero; the remaining volume integral takes the form

$$\int_{V-V_0} dV\,[\mathbf{v}\cdot\mathbf{f}] = \hat{\mathbf{x}}_k\cdot\mathbf{v}(\mathbf{r}) \tag{30}$$

(as long as the position $\mathbf{r}$ of the unit point force $\mathbf{f}$ is within $V - V_0$). The surface integrals over the exterior surface ∂V of the Earth model vanish because of the boundary conditions (28) and (29). Now let the volume V_0 shrink to zero and let the closed surface ∂V_0 collapse to become the surface area Σ_0 of an earthquake fault (see Fig. 1). The surface integral over the surface ∂V_0 becomes a surface integral over the surface Σ_0, a fault surface located within the volume V of the Earth model, and (27) takes the form

$$\hat{\mathbf{x}}_k.\mathbf{v}(\mathbf{r}) = \int_{\Sigma_0} dS_0\, n_j^0 \left\{E_{ij}\,[v_i]_-^+ + \left(\frac{1}{4\pi G}\,\partial_j\phi_1 + \rho_0\,u_j\right)[\psi_1]_-^+ - u_i[D_{ij}]_-^+ - \phi_1\left[\frac{1}{4\pi G}\,\partial_j\psi_1 + \rho_0\,v_j\right]_-^+\right\}. \tag{31}$$

In equation (31) quantities such as $[v_i]_-^+$ represent jump discontinuities across the fault surface Σ_0.

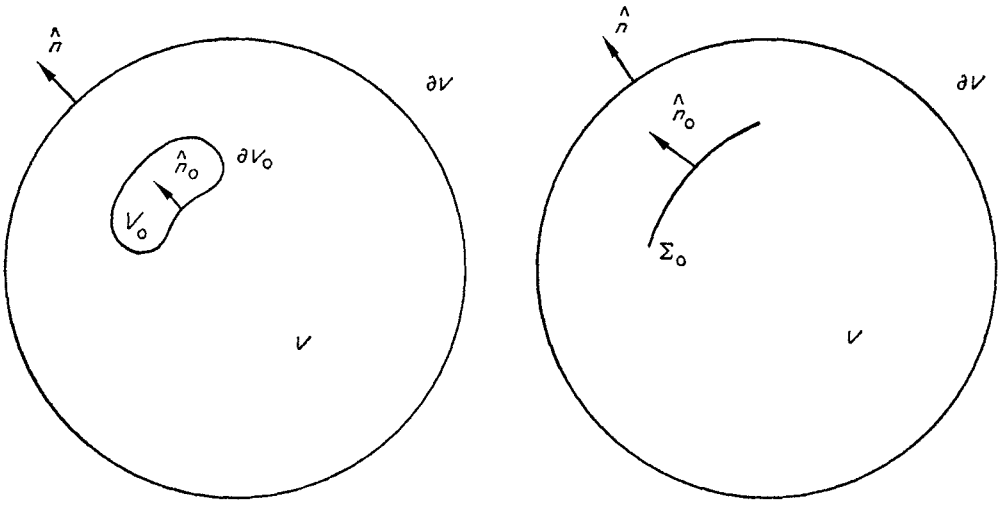

FIG. 1. Schematic view of an Earth model V with an imaginary closed internal surface ∂V_0 and with an arbitrary fault surface Σ_0.

It is convenient at this point to clarify the notation slightly. Let $\Delta\mathbf{v}(\mathbf{r}_0) = [\mathbf{v}(\mathbf{r}_0)]^+_-$ stand for a jump discontinuity in the displacement field across the fault surface Σ_0. Points located on the fault surface will be denoted by $\mathbf{r}_0$. If the normal $\hat{\mathbf{n}}_0$ to the surface Σ_0 points out of the positive side of Σ_0, then $\Delta\mathbf{v}(\mathbf{r}_0)$ is the jump discontinuity in going from the positive to the negative side of Σ_0. Let $E_{ij}{}^k(\mathbf{r}, \mathbf{r}_0)$ denote the elastic stress produced at the point $\mathbf{r}_0$ on the fault surface Σ_0 by the unit point force $\mathbf{f}$ located at $\mathbf{r}$ and pointing in the direction $\hat{\mathbf{x}}_k$. Utilizing this clearer notation, equation (31) takes the form

$$v_k(\mathbf{r}) = \int_{\Sigma_0} dS_0\, n_j{}^0 \left\{ E_{ij}{}^k(\mathbf{r}, \mathbf{r}_0)\, \Delta v_i(\mathbf{r}_0) + \left[\frac{1}{4\pi G}\, \partial_j \phi_1{}^k(\mathbf{r}, \mathbf{r}_0) + \rho_0\, u_j{}^k(\mathbf{r}, \mathbf{r}_0) \right] \Delta\psi_1(\mathbf{r}_0) \right.$$

$$\left. - u_i{}^k(\mathbf{r}, \mathbf{r}_0)\, \Delta D_{ij}(\mathbf{r}_0) - \frac{1}{4\pi G}\, \phi_1{}^k(\mathbf{r}, \mathbf{r}_0)\, \Delta \left[\partial_j \psi_1(\mathbf{r}_0) + 4\pi G \rho_0\, v_j(\mathbf{r}_0) \right] \right\}. \quad (32)$$

Equation (32) provides an explicit formula which allows one to compute the elastic-gravitational displacement $\mathbf{v}(\mathbf{r})$ at an arbitrary point $\mathbf{r}$ within the Earth model V in terms of certain prescribed discontinuities across a fault surface Σ_0 embedded within V_0. The question of which discontinuities may be prescribed independently in an elastic dislocation problem is discussed by Burridge & Knopoff (1964) for the case of a non-gravitating elastic medium. It will be assumed without proof here that from the point of view of mathematical consistency, the following jump discontinuities may all be specified independently on the fault surface:

$$\Delta\mathbf{v},\ \Delta\psi_1,\ \hat{\mathbf{n}}_0 \cdot \Delta\mathbf{D},\ \hat{\mathbf{n}}_0 \,.\, \Delta[\nabla\psi_1 + 4\pi G\rho_0\, \mathbf{v}]\,.$$

In other words, equation (32) represents a complete solution to the elastic-gravitational problem with prescribed jump discontinuities on a fault surface Σ_0, since all of the jump discontinuities which appear in (32) may be prescribed independently.

Consider the case where only the jump discontinuity in displacement $\Delta\mathbf{v}(\mathbf{r}_0)$ is specified to be non-zero, i.e. on Σ_0

$$\left.\begin{aligned} \Delta\psi_1 &= 0 \\ \hat{\mathbf{n}}_0 . \Delta\mathbf{D} &= 0 \\ \hat{\mathbf{n}}_0 . \Delta[\nabla\psi_1 + 4\pi G\rho_0 \mathbf{v}] &= 0. \end{aligned}\right\} \tag{33}$$

In that case (32) reduces to

$$v_k(\mathbf{r}) = \int_{\Sigma_0} dS_0 \, n_j^0 [E_{ij}^k(\mathbf{r}, \mathbf{r}_0) \, \Delta v_i(\mathbf{r}_0)]. \tag{34}$$

Equation (34) is the fundamental relation of elastic dislocation theory, sometimes called the Volterra relation (Volterra 1907; Skeketee 1958; Maruyama 1963, 1964). The above derivation shows that Volterra's relation is valid for an arbitrary fault surface Σ_0 located in an arbitrary self-gravitating SNREI Earth model. In fact, since the Betti reciprocal theorem (26) can be shown to be valid even for any non-SNREI self-gravitating elastic configuration, it is clear that Volterra's relation (34) too is valid for any non-SNREI Earth model. As far as I know, previous derivations of Volterra's relation have never considered explicitly the effect of self-gravitation, although Singh & Ben-Menahem (1969) utilized Volterra's relation in their discussion of internal dislocations in a homogeneous self-gravitating sphere.

If the discontinuity in displacement or the slip $\Delta\mathbf{v}(\mathbf{r}_0)$ on a fault surface Σ_0 in a SNREI Earth model V is known, then Volterra's relation provides an explicit determination of the accompanying static elastic displacement $\mathbf{v}(\mathbf{r})$ at any other point $\mathbf{r}$ in the Earth model. The stress kernels $E_{ij}^k(\mathbf{r}, \mathbf{r}_0)$ in Volterra's relation may be shown to be the components of a third order tensor which may be called the Green's tensor. The Green's tensor components $E_{ij}^k(\mathbf{r}, \mathbf{r}_0)$ may be determined if one can compute the elastic-gravitational response of the SNREI Earth model V to an applied unit point body force $\mathbf{f}$ located at $\mathbf{r}$.

For simplicity, consider a fault surface Σ_0 which is small compared to the overall size of the Earth model. In that case the surface integration over Σ_0 in Volterra's relation may be approximated by

$$v_k(\mathbf{r}) = A_0 [n_j^0 \, E_{ij}^k(\mathbf{r}, \mathbf{r}_0) \, \overline{\Delta v_i}(\mathbf{r}_0)] \tag{35}$$

where A_0 is the area of the fault surface Σ_0 and $\overline{\Delta\mathbf{v}}$ is the average slip on the fault. Writing $\overline{\Delta\mathbf{v}} = \overline{\Delta v}\hat{\mathbf{e}}_0$ where $\hat{\mathbf{e}}_0$ is a unit vector in the direction of slip, (35) becomes

$$v_k(\mathbf{r}) = [A_0 \, \overline{\Delta v_0}][n_j^0 \, e_i^0 \, E_{ij}^k(\mathbf{r}, \mathbf{r}_0)] \tag{36}$$

or rewritten in invariant notation

$$v_k(\mathbf{r}) = [A_0 \, \overline{\Delta v_0}) \, tr \, [\hat{\mathbf{n}}_0 \, \hat{\mathbf{e}}_0 . \mathbf{E}^k(\mathbf{r}, \mathbf{r}_0)]. \tag{37}$$

Equation (37) is Volterra's relation for a point displacement dislocation. Burridge & Knopoff (1964) have used a dynamical form of this relation (37) to show that a point displacement dislocation source is dynamically equivalent to a double-couple source.

In this paper the static effect of an earthquake in the Earth will be modelled in terms of the elastic-gravitational response of a specified SNREI Earth model to a static tangential point displacement dislocation at the earthquake hypocentre A tangential dislocation is one in which the slip vector $\hat{\mathbf{e}}_0$ is perpendicular to the fault plane normal $\hat{\mathbf{n}}_0$. It will be seen that neglect of the finite dimensions of an earthquake fault surface is perfectly justifiable in view of the many other large uncertainties

which arise in the computation. Equation (37) shows that the static elastic-gravitational response of a SNREI Earth model V to an internal point displacement dislocation may be written as the product of two terms The first term $[A_0\,\overline{\Delta v}_0]$ is a measure of the size of the earthquake fault displacement which is being modelled by the point displacement dislocation. This term $[A_0\,\Delta v_0]$ is the area of the fault surface multiplied by the average tangential slip on the fault and may be called the earthquake slip-area The earthquake slip-area is closely related to the earthquake moment defined by Brune (1968) (see Section 4). The second term.

$$tr[\hat{\mathbf{n}}_0\,\hat{\mathbf{e}}_0\cdot\mathbf{E}^k(\mathbf{r},\mathbf{r}_0)]$$

depends on the location $\mathbf{r}_0$ and on the geometry and orientation $\hat{\mathbf{n}}_0, \hat{\mathbf{e}}_0$ of the earthquake fault as well as on the particular SNREI Earth model under consideration, since $\mathbf{E}^k(\mathbf{r}, \mathbf{r}_0)$ is a function of the response of the Earth model to a unit point force $\mathbf{f}$ at $\mathbf{r}$. It is interesting to note in passing that $tr[\hat{\mathbf{n}}_0\,\hat{\mathbf{e}}_0 . E^k]$ is symmetric in $\hat{\mathbf{n}}_0$ and $\hat{\mathbf{e}}_0$ since the stress $\mathbf{E}^k$ is a symmetric second order tensor for fixed k. This means that if the fault plane normal $\hat{\mathbf{n}}_0$ and the slip vector $\hat{\mathbf{e}}_0$ of a point fault source are interchanged, the resultant static strain field $\mathbf{v}(\mathbf{r})$ in the Earth is unchanged. This is analogous to the ambiguity between the fault plane and the auxiliary plane which arises in a P wave first motion focal mechanism solution (Hodgson 1957).

Before showing how the term $tr(\hat{\mathbf{n}}_0\,\hat{\mathbf{e}}_0\cdot\mathbf{E}^k)$ may be evaluated for a particular SNREI Earth model, it may be worthwhile to discuss some seemingly peculiar features of the assumptions which are made in utilizing elastic dislocation theory for a SNREI Earth model for this application. Note first of all that one clearly cannot use a SNREI Earth model as a model of the Earth in discussing the Chandler wobble itself. It would be meaningless to consider the Eulerian nutation of a nonrotating configuration; furthermore, the aspherical shape of the rotating Earth plays an essential rose in the dynamics of the Chandler wobble. It is however perfectly justifiable to utilize a non-rotating, spherically symmetric Earth model in order to compute the static elastic-gravitational displacement field associated with the slip on an earthquake fault. Neglect of rotation implies neglect of the centrifugal force term in the static elastic-gravitational equations (17); this will give rise to errors of order $\Omega^2 a^3/GM$, where M is the mass of the Earth and a is the mean radius (the quantity $\Omega^2 a^3/GM$ is essentially the ratio of the equatorial centrifugal force to the equatorial gravitational force on the Earth's surface). Neglect of the aspherical shape of the Earth will give rise to errors of order ε_a, where ε_a is the surface ellipticity of the Earth. Both ε_a and $\Omega^2 a^3/GM$ are about one part in 300 and thus quite negligible for this application. Another assumption which warrants examination is the neglect in the static elastic-gravitational equations (17) of any pre-existing static non-hydrostatic stress field. An earthquake in the real Earth is generally considered to represent a sudden release through material failure of some kind of a slowly accumulating non-hydrostatic stress field. The existence in the Earth of non-hydrostatic stresses is an essential element of the dynamics of the earthquake process. The use of elastic dislocation theory however enables one to avoid completely any consideration of the dynamics of the earthquake mechanism. The description of an earthquake source in elastic dislocation theory is purely kinematical (i.e. the slip on a fault surface). Given the slip on the fault surface, one can compute the resultant static displacement field and thus the resultant static stress field at all other points in the Earth model. In fact, the static stress field which one computes using elastic dislocation theory is the inverse or negative of the static non-hydrostatic stress actually released by the earthquake. This is because the introduction in the Earth model of a displacement dislocation on a fault surface Σ_0 implies the action of applied stresses on Σ_0. These stresses which one must apply to Σ_0 in order to produce the observed slip are the inverse or negative of the stresses actually released on Σ_0

by the earthquake. The utilization of a SNREI Earth model in the elastic dislocation computation implies the assumption that the static non-hydrostatic stress fields existing in the Earth before the earthquake and partially released by the earthquake are small compared to the hydrostatic stresses in the Earth. Since this seems to be the case (Jeffreys 1963; MacDonald 1966), the use of a SNREI Earth model is perfectly adequate to compute earthquake-associated static displacements and stress release fields so long as one is content to avoid discussion of the dynamics of the earthquake mechanism.

Consider now the evaluation of the changes in the inertia tensor ΔC of a SNREI Earth model which are produced as a result of the static displacement fields accompanying an earthquake. The static displacement field $\mathbf{v}(\mathbf{r})$ for a point tangential displacement dislocation may be computed from equation (37). Because of the spherical symmetry of a SNREI Earth model, it is convenient to express the vector field $\mathbf{v}(\mathbf{r})$ in terms of its scalar potential expansion (Backus 1967),

$$\mathbf{v}(\mathbf{r}) = \hat{\mathbf{r}}\mathscr{U}(r,\theta,\phi) + \nabla_1 \mathscr{V}(r,\theta,\phi) - \hat{\mathbf{r}} \times \nabla_1 \mathscr{W}(r,\theta,\phi) \tag{38}$$

where

$$\nabla_1 = \hat{\boldsymbol{\theta}} \frac{\partial}{\partial \theta} + \hat{\boldsymbol{\phi}} \frac{1}{\sin\theta} \frac{\partial}{\partial \phi} .$$

In (38), $\hat{\mathbf{r}}$, $\hat{\boldsymbol{\theta}}$, $\hat{\boldsymbol{\phi}}$ define a geographic spherical coordinate system related to the previously defined geographic Cartesian axes $\hat{\mathbf{x}}_1$, $\hat{\mathbf{x}}_2$, $\hat{\mathbf{x}}_3$ in the usual manner (θ is the colatitude, ϕ is the longitude east from Greenwich). It can be shown that the three scalar potential fields $\mathscr{U}$, $\mathscr{V}$, $\mathscr{W}$ in (38) are unique. Each of these scalar fields $\mathscr{U}$ $\mathscr{V}$, $\mathscr{W}$ may be expanded in surface spherical harmonics $Y_l^m(\theta,\phi)$. In this paper $Y_l^m(\theta,\phi)$ represents the fully normalized complex surface spherical harmonic

$$Y_l^m(\theta,\phi) = (-1)^m \left[\frac{2l+1}{4\pi}\right]^{\frac{1}{2}} \left[\frac{(l-m)!}{(l+m)!}\right]^{\frac{1}{2}} P_l^m(\cos\theta) \exp(im\phi). \tag{39}$$

The normalization is such that

$$\int_S Y_l^m \overset{*}{Y}_l^m \, d\Omega = 1 \tag{40}$$

where S is the surface of the unit sphere. It is somewhat more convenient here to avoid using negative values of m by defining

$$Y_l^m = A_l^m + iB_l^m \tag{41}$$

so that one can write the spherical harmonic expansions of $\mathscr{U}$, $\mathscr{V}$, $\mathscr{W}$ in the form

$$\left.\begin{aligned}
\mathscr{U}(r,\theta,\phi) &= \sum_{l=0}^{\infty} \left\{ \mathscr{U}_l^0(r) A_l^0(\theta,\phi) + 2\sum_{m=1}^{l} [\mathscr{U}_l^m(r) A_l^m(\theta,\phi) + \tilde{\mathscr{U}}_l^m(r) B_l^m(\theta,\phi)] \right\} \\
\mathscr{V}(r,\theta,\phi) &= \sum_{l=0}^{\infty} \left\{ \mathscr{V}_l^0(r) A_l^0(\theta,\phi) + 2\sum_{m=1}^{l} [\mathscr{V}_l^m(r) A_l^m(\theta,\phi) + \tilde{\mathscr{V}}_l^m(r) B_l^m(\theta,\phi)] \right\} \\
\mathscr{W}(r,\theta,\phi) &= \sum_{l=0}^{\infty} \left\{ \mathscr{W}_l^0(r) A_l^0(\theta,\phi) + 2\sum_{m=1}^{l} [\mathscr{W}_l^m(r) A_l^m(\theta,\phi) + \tilde{\mathscr{W}}_l^m(r) B_l^m(\theta,\phi)] \right\} .
\end{aligned}\right\} \tag{42}$$

The inertia tensor $\mathbf{C}$ of a mass configuration $\rho(\mathbf{r})$ occupying a volume is defined as

$$\mathbf{C} = \int_V \rho(\mathbf{r})[(\mathbf{r}\cdot\mathbf{r})\,\mathbf{I} - \mathbf{rr}]\,dV \tag{43}$$

where $\mathbf{I}$ is the second order identity tensor. The change $\Delta\mathbf{C}$ in the inertia tensor of an Earth model V produced by an earthquake static displacement field $\mathbf{v}(\mathbf{r})$ is thus given by

$$\Delta\mathbf{C} = \int_{V_1} \rho_1(\mathbf{r})[(\mathbf{r}\cdot\mathbf{r})\,\mathbf{I} - \mathbf{rr}]\,dV \tag{44}$$

where $\rho_1(\mathbf{r})$ is the change in density at the point $\mathbf{r}$ associated with the static displacement, and where V_1 is the deformed volume V. It has been mentioned that the change in density $\rho_1(\mathbf{r})$ is related to $\mathbf{v}(\mathbf{r})$ through the linearized continuity equation

$$\rho_1(\mathbf{r}) = -\nabla\cdot[\rho_0\,\mathbf{v}(\mathbf{r})]. \tag{45}$$

Utilizing the scalar expansion (38) of $\mathbf{v}(\mathbf{r})$ one can thus write

$$\rho_1(r,\theta,\phi) = \sum_{l=0}^{\infty}\left\{\mathscr{D}_l^0(r)\,A_l^0(\theta,\phi) + 2\sum_{m=1}^{l}[\mathscr{D}_l^m(r)\,A_l^m(\theta,\phi) + \tilde{\mathscr{D}}_l^m(r)\,B_l^m(\theta,\phi)]\right\} \tag{46}$$

where

$$\left.\begin{aligned}\mathscr{D}_l^m(r) &= -\rho_0\left[\partial_r\,\mathscr{U}_l^m(r) + \frac{2}{r}\,\mathscr{U}_l^m(r) - \frac{l(l+1)}{r}\,\mathscr{V}_l^m(r)\right] - \partial_r\rho_0\,\mathscr{U}_l^m(r)\\ \tilde{\mathscr{D}}_l^m(r) &= -\rho_0\left[\partial_r\,\tilde{\mathscr{U}}_l^m(r) + \frac{2}{r}\,\tilde{\mathscr{U}}_l^m(r) - \frac{l(l+1)}{r}\,\tilde{\mathscr{V}}_l^m(r)\right] - \partial_r\rho_0\,\tilde{\mathscr{U}}_l^m(r).\end{aligned}\right\} \tag{47}$$

Note that there is no change in density associated with the toroidal part of the displacement field $\mathbf{v}(\mathbf{r})$.

Note that the volume integration in equation (44) is to be performed over the deformed volume V_1. In fact it can be shown that to first order in $\mathbf{v}(\mathbf{r})$, volume integration over V_1 is equivalent to volume integration over the undeformed spherical volume V so long as the displacement of every spherical surface across which there is a jump discontinuity in $\rho_0(r)$ (e.g. the exterior surface $r = a$) is taken into account by recalling that $\partial_r\rho_0(r)$ will include a delta function contribution at that radius. There will also be a delta function contribution at the level $r = r_0$, due to the fact that $\mathbf{v}(\mathbf{r})$ and thus $\mathscr{U}_l^m(r)$ and $\tilde{\mathscr{U}}_l^m(r)$ are discontinuous at the source.

Now consider the volume integration in (44) performed over the spherical volume of a SNREI Earth model V. If the order of integration and summation are interchanged, one obtains a spherical harmonic expansion for the components of $\Delta\mathbf{C}$. However, due to the orthogonality relations between surface spherical harmonics Y_l^m, all the terms in the expansion for $\Delta\mathbf{C}$ disappear with the exception of $l = 2$. The final expressions for the components ΔC_{13} and ΔC_{23} are

$$\left.\begin{aligned}\Delta C_{13} &= \sqrt{\left[\frac{8\pi}{15}\right]}\int_0^a dr[r^4\,\mathscr{D}_2^1(r)]\\ \Delta C_{23} &= \sqrt{\left[\frac{8\pi}{15}\right]}\int_0^a dr[r^4\,\tilde{\mathscr{D}}_2^1(r)].\end{aligned}\right\} \tag{48}$$

In order to determine the effect of an individual earthquake on the motion of the pole of rotation, one must compute the changes ΔC_{13} and ΔC_{23} in the inertia tensor

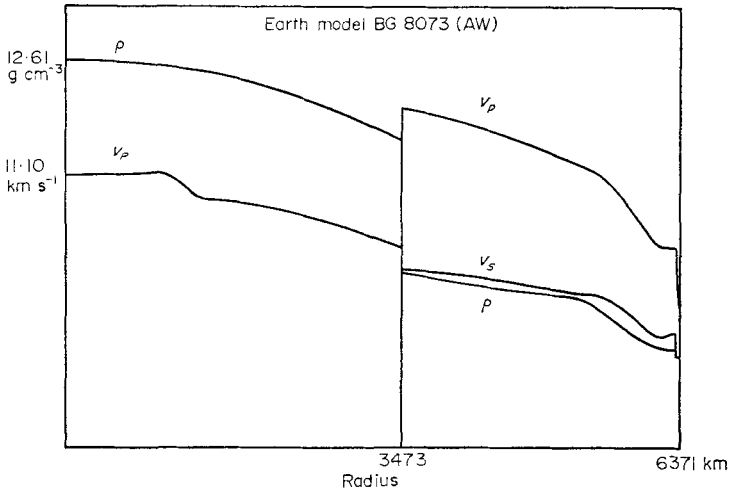

FIG. 2. Plot of $v_p(r)$, $v_s(r)$, $\rho(r)$ for SNREI Earth model 8073AW. This SNREI Earth model was used for numerical computations.

components But to compute ΔC_{13} and ΔC_{23} it is only necessary to compute four vector spherical harmonic components of the static displacement field $\mathbf{v}(\mathbf{r})$, namely $\mathscr{U}_2{}^1(r)$, $\mathscr{V}_2{}^1(r)$, $\tilde{\mathscr{U}}_2{}^1(r)$, $\tilde{\mathscr{V}}_2{}^1(r)$. Note that if one wishes to compute the entire static displacement field $\mathbf{v}(\mathbf{r})$ it is necessary to evaluate a vector spherical harmonic sum (42).

It is shown in Appendices 1 and 2 how Volterra's relation (37) may be used to compute the scalar radial functions $\mathscr{U}_2{}^1(r)$, $\mathscr{V}_2{}^1(r)$, $\tilde{\mathscr{U}}_2{}^2(r)$, $\tilde{\mathscr{V}}_2{}^1(r)$ for an arbitrary point tangential displacement dislocation in an arbitrary SNREI Earth model. In this section only the final results of the actual numerical computation for a particular SNREI Earth model are presented. The SNREI Earth model which has been used for the numerical computations is shown in Fig. 2. This is model 8073 of Backus & Gilbert (tabulated in Slichter 1967), except that the density profile $\rho_0(r)$ in the fluid core has been slightly modified to satisfy an Adams–Williamson criterion (see Appendix B). This SNREI Earth model (call it 8073AW) has no solid inner core; it does have Moho discontinuity at a depth of 28 km and it does have a low shear velocity zone.

It is convenient for the purposes of discussion to define the geometry of an arbitrary point tangential displacement dislocation not in terms of the fault plane normal $\hat{\mathbf{n}}_0$ and slip vector $\hat{\mathbf{e}}_0$ but in terms of the more customary fault parameters. Fig. 3 shows how this is done. The location of an arbitrary earthquake is given by its colatitude θ_0, its longitude east of Greenwich ϕ_0, and its distance from the Earth's centre r_0 (or equivalently its depth $h = a - r_0$). The fault plane is customarily defined by its strike azimuth α on the Earth's surface (measured here counterclockwise from north) and its dip δ with respect to the Earth's surface. The one remaining quantity which can be used to specify completely the nature of an arbitrary point tangential displacement dislocation is the slip angle λ measured in the fault plane counterclockwise from the horizontal. The unit vectors $\hat{\mathbf{n}}_0$ and $\hat{\mathbf{e}}_0$ can be expressed in terms of the strike α, dip δ, and slip λ of the fault in the following way (Ben-Menahem & Singh 1968)

$$\left.\begin{aligned}
\hat{\mathbf{n}}_0 &= \cos\delta\hat{\mathbf{r}}_0 + \sin\alpha\,\sin\delta\hat{\boldsymbol{\theta}}_0 - \cos\alpha\,\sin\delta\hat{\boldsymbol{\phi}}_0 \\
\hat{\mathbf{e}}_0 &= \sin\delta\,\sin\lambda\hat{\mathbf{r}}_0 + (\cos\alpha\,\cos\lambda - \sin\alpha\,\cos\delta\,\sin\lambda)\,\hat{\boldsymbol{\theta}}_0 \\
&\qquad + (\sin\alpha\,\cos\lambda + \cos\alpha\,\cos\delta\,\sin\lambda)\,\hat{\boldsymbol{\phi}}_0 \\
\hat{\mathbf{n}}_0 \cdot \hat{\mathbf{e}}_0 &= 0.
\end{aligned}\right\} \tag{49}$$

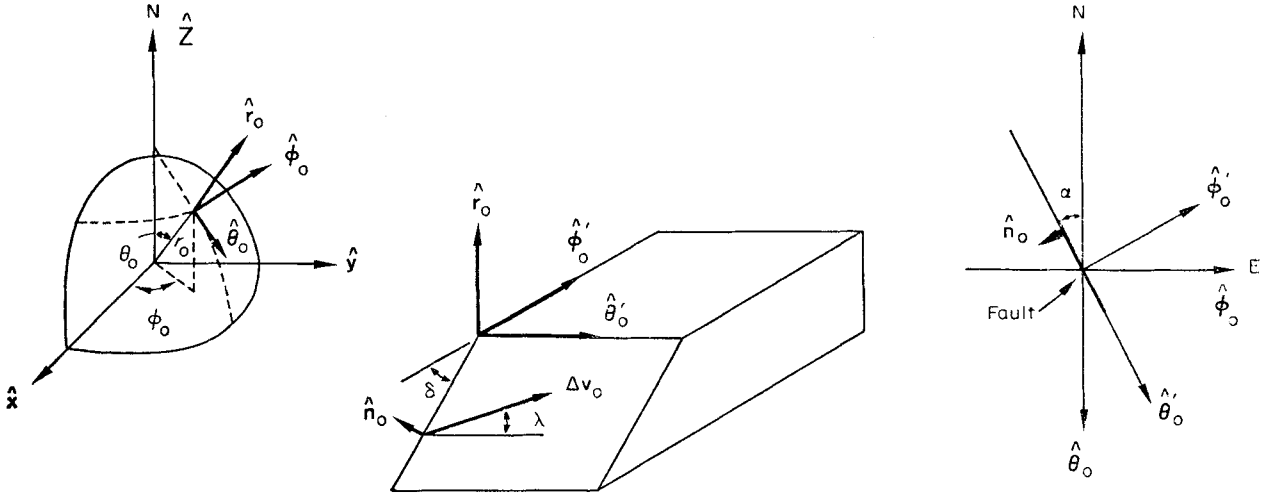

FIG. 3. Diagrams showing definition of fault parameters h, θ_0, ϕ_0, α, δ, λ. Left-hand diagram shows definition of fault location h, θ_0, ϕ_0 in spherical geocentric co-ordinate system ($h = a - r_0$); right-hand diagram is map view of Earth's surface showing definition of fault plane strike azimuth a; middle diagram is perspective cutaway view of fault surface showing δ and λ.

The unit vectors $\hat{\boldsymbol{\theta}}_0'$ and $\hat{\boldsymbol{\phi}}_0'$ are in the plane of the Earth's surface and are, respectively, parallel and perpendicular to the fault strike.

Utilizing the expressions (49) for $\hat{\mathbf{n}}_0$ and $\hat{\mathbf{e}}_0$ in terms of α, δ, λ, one can proceed to use Volterra's relation (37) to determine $\mathscr{U}_2{}^1(r)$, $\mathscr{V}_2{}^1(r)$, $\tilde{\mathscr{U}}_2{}^1(r)$, $\tilde{\mathscr{V}}_2{}^1(r)$ and then to evaluate the integrals (48) in order to determine the changes ΔC_{13} and ΔC_{23} due to an arbitrary earthquake in terms of the earthquake fault plane location h, θ_0, ϕ_0 and orientation α, δ, λ. The algebraic details of this evaluation have been placed in Appendices 1 and 2. It is shown there that the expressions (48) for ΔC_{13} and ΔC_{23} can be written finally in the form

$$\left.\begin{aligned}
\Delta C_{13} = {} & [A_0\,\overline{\Delta v_0}]\{\Gamma_1(h)[(\sin 2\alpha \sin\delta \cos\lambda + \tfrac{1}{2}\cos 2\alpha \sin 2\delta \sin\lambda)\sin 2\theta_0 \cos\phi_0 \\
& -2(\tfrac{1}{2}\sin 2\alpha \sin 2\delta \sin\lambda - \cos 2\alpha \sin\delta \cos\lambda)\sin\theta_0 \sin\phi_0] \\
& +\Gamma_2(h)[-\sin 2\delta \sin\lambda \sin 2\theta_0 \cos\phi_0] \\
& +\Gamma_3(h)[(\sin\alpha \cos 2\delta \sin\lambda - \cos\alpha \cos\delta \cos\lambda)\cos 2\theta_0 \cos\phi_0 \\
& +(\sin\alpha \cos\delta \cos\lambda + \cos\alpha \cos 2\delta \sin\lambda)\cos\theta_0 \sin\phi_0]\} \\
\Delta C_{23} = {} & [A_0\,\overline{\Delta v_0}]\{\Gamma_1(h)[(\sin 2\alpha \sin\delta \cos\lambda + \tfrac{1}{2}\cos 2\alpha \sin 2\delta \sin\lambda)\sin 2\theta_0 \sin\phi_0 \\
& +2(\tfrac{1}{2}\sin 2\alpha \sin 2\delta \sin\lambda - \cos 2\alpha \sin\delta \cos\lambda)\sin\theta_0 \cos\phi_0] \\
& +\Gamma_2(h)[-\sin 2\alpha \sin\lambda \sin 2\theta_0 \sin\phi_0] \\
& +\Gamma_3(h)[(\sin\alpha \cos 2\delta \sin\lambda - \cos\alpha \cos\delta \cos\lambda)\cos 2\theta_0 \sin\phi_0 \\
& -(\sin\alpha \cos\delta \cos\lambda + \cos\alpha \cos 2\delta \sin\lambda)\cos\theta_0 \cos\phi_0]\}.
\end{aligned}\right\} \quad (50)$$

In (50), the dependence of ΔC_{13} and ΔC_{23} due to an earthquake on the angular fault parameters θ_0, ϕ_0, α, δ, λ has been explicitly indicated. The three functions of earthquake depth $\Gamma_1(h)$, $\Gamma_2(h)$, $\Gamma_3(h)$ depend on the SNREI Earth model used in the numerical computations. The three functions $\Gamma_1(h)$, $\Gamma_2(h)$, $\Gamma_3(h)$ for the model 8073 AW are shown in Fig. 4. It is clear from Fig. 4 that earthquake-induced changes in the inertia tensor of SNREI Earth model 8073 AW are not severely dependent on the depth of the earthquake. The small wiggle in $\Gamma_2(h)$ at a depth of about 30 km is caused by the presence of a Moho discontinuity in SNREI Earth model 8073 AW.

Ben-Menahem & Israel (1970) have shown how to compute ΔC_{13} and ΔC_{23} for a point tangential displacement dislocation in a homogeneous non-gravitating Earth

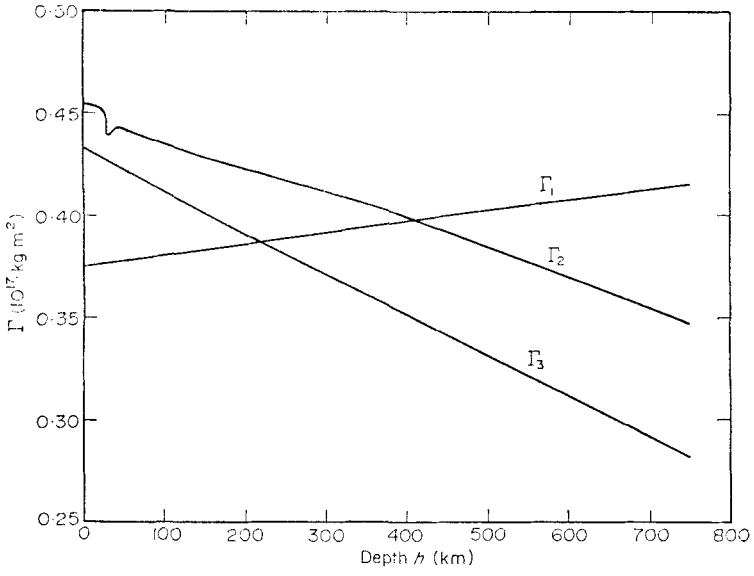

FIG. 4. Plot of $\Gamma_1(h)$, $\Gamma_2(h)$, $\Gamma_3(h)$ for SNREI Earth model 8073AW.

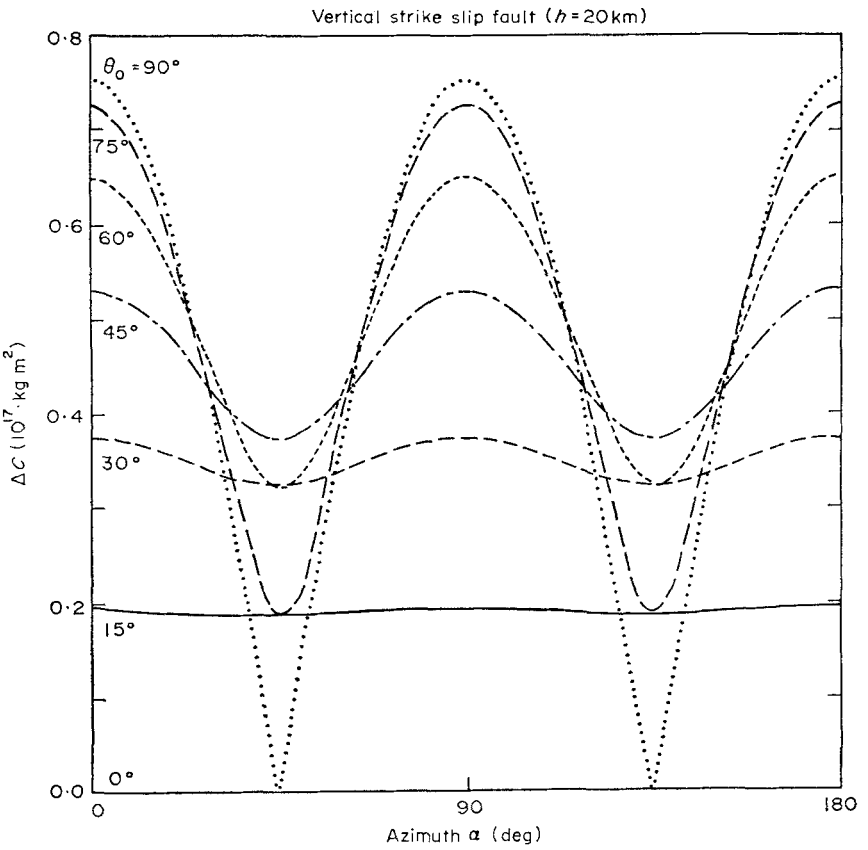

FIG. 5. Plot showing variation of $\Delta C = (\Delta C^2_{13} + \Delta C^2_{23})^{\frac{1}{2}}$ with respect to fault strike α and colatitude θ_0 for a vertical strike slip fault of unit slip-area ($A_0\,\overline{\Delta v}_0$).

model. Using quite a different algebraic development of Volterra's relation (37), they deduced a relation similar to (50). The explicit dependence of ΔC_{13} and ΔC_{23} on the angular variables deduced by Ben-Menahem & Israel was identical to that in (50), but the functions $\Gamma_1(h)$, $\Gamma_2(h)$, $\Gamma_3(h)$ are of course different for a homogeneous, non-gravitating Earth model. Ben-Menahem & Israel (1970) chose to present their results in terms of three canonical fault model types rather than in terms of three radial functions $\Gamma_1(h)$, $\Gamma_2(h)$, $\Gamma_3(h)$. For example, examination of (50) reveals that vertical strike slip fault models ($\delta = 90°$, $\lambda = 0°$) depend only on $\Gamma_1(h)$ whereas vertical dip slip fault models ($\delta = 90°$, $\lambda = 90°$) depend only on $\Gamma_3(h)$.

Knowing $\Gamma_1(h)$, $\Gamma_2(h)$, $\Gamma_3(h)$ for a SNREI Earth model, one can use (50) to compute ΔC_{13} and ΔC_{23} caused by an earthquake of arbitrary location and arbitrary fault geometry. Figs 5 and 6 give some examples of the manner in which the changes in the inertia tensor ΔC_{13} and ΔC_{23} depend upon fault location and orientation. Fig. 5 is a plot of $\Delta C = (\Delta C_{23}{}^2 + \Delta C_{23}{}^2)^{\frac{1}{2}}$ versus fault strike azimuth for various values of earthquake co-latitude θ_0 for a shallow vertical strike-slip fault mechanism ($\delta = 90°$, $\lambda = 0°$, $h = 20$ km). The scale of the ordinate is such that the fault is considered to have unit slip-area [$A_0\,\overline{\Delta v}_0$]. Vertical shallow strike slip faulting is the type which is prevalent on continental transcurrent faults (such as the San Andreas Fault) and on oceanic transform faults (Sykes 1967); i.e. wherever one lithospheric plate is slipping past another. Fig. 6 is a similar diagram for a shallow angle thrust or

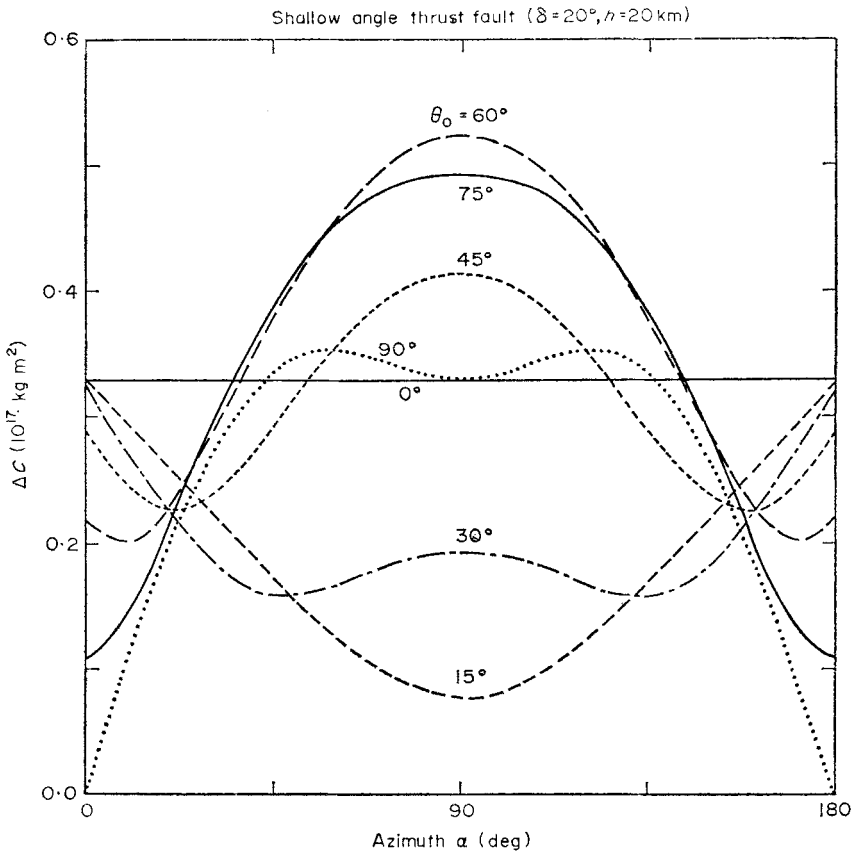

FIG. 6. Plot showing variation of $\Delta C = (\Delta C^2_{13} + \Delta C^2_{23})^{\frac{1}{2}}$ with respect to fault strike α and co-latitude θ_0 for a shallow angle ($\delta = 20°$) thrust fault of unit slip-area.

dip slip fault mechanism ($\delta = 20°$, $\lambda = 90°$, $h = 20$ km). Shallow angle thrust faulting predominates in oceanic trench and island arc regions where one lithospheric plate is plunging beneath another (Stauder & Bollinger 1966; Isacks, Oliver & Sykes 1968). It is evident from Figs 5 and 6 that the extent to which a particular earthquake changes the inertia tensor components ΔC_{13} and ΔC_{23} depends critically on the location and the geometry of the associated earthquake faulting.

Equation (50) allows one to compute ΔC_{13} and ΔC_{23} for SNREI Earth model 8073 AW produced by an arbitrary earthquake event if the six earthquake fault parameters h, θ_0, ϕ_0, α, δ, λ can be specified. In Section 4, equation (50) is applied to two specific cases, the 1960 Chilean earthquake and the 1964 Alaskan earthquake. In Section 5 it is shown how equation (50) is actually utilized in this paper to estimate the total Chandler wobble power produced by all past earthquakes.

4. Chilean earthquake 1960 and Alaskan earthquake 1964

The major difficulty in using the theory of Section 3 to compute the inertia tensor changes produced by an earthquake is that one requires as input considerable information about the nature of the faulting associated with the earthquake. In order to use equation (50) to compute ΔC_{13} and ΔC_{23} produced by an arbitrary earthquake, one must be able to specify the fault slip-area $[A_0 \overline{\Delta v_0}]$, the earthquake location h, θ_0, ϕ_0, and the fault plane geometry α, δ, λ. There are many varied kinds of in-

formation which can be used to determine the size and nature of the faulting mechanism associated with any particular past large earthquake. There are however very few past large earthquakes which have been really intensively studied and for which both the total slip-area $[A_0\,\overline{\Delta v}_0]$ and the faulting mechanism may be considered well known.

Two recent earthquakes which have been intensively studied are the Chilean earthquake of 1960 May 22 and the Alaskan earthquake of 1964 March 27. These are the two largest earthquakes which have occurred in the past decade. For both of these earthquakes, all of the data which is available combine to give a fairly consistent picture of the nature and size of the associated faulting mechanism.

A particularly effective method of investigating the nature of the faulting associated with a large earthquake is to utilize measurements of ground deformation in the vicinity of the earthquake. Measurements of local ground deformation may be made by comparison of survey networks before and after the earthquake, by comparison of tide gauge readings before and after the earthquake, or by utilizing geological evidence such as uplifted shorelines, etc. If measurements of the localized ground deformation are reasonably complete, then reliable inferences can be made concerning the finite size, location, and attitude of the fault surface and the direction and magnitude of slip as a function of position on the fault surface. The local ground deformation associated with both the 1960 Chilean earthquake and the 1964 Alaskan earthquake has been fairly well determined; the results for the 1960 Chilean earthquake have been summarized by Plafker & Savage (1970) and for the 1964 Alaskan earthquake by Plafker (1969). In both of these cases, a unique interpretation was hindered by the fact that these are oceanic trench earthquakes and the region of greatest ground deformation lies underwater where it cannot be observed. It is clear however that in both cases the measurements of local ground deformation agree best with the hypothesis that the faulting is thrust faulting on a fault plane dipping at a shallow or moderate angle. In both cases this is exactly the type of faulting which is predicted by the hypothesis of lithospheric plate tectonics (Morgan 1968; Isacks *et al.* 1968). The 1960 Chilean earthquake is associated with the thrusting of the Nazca plate under the American plate in the Peru–Chile trench, and the 1964 Alaskan earthquake is associated with the thrusting of the Pacific plate under the American plate in the Aleutian trench. Stauder & Bollinger (1966) have made P-wave first motion focal mechanism studies of the 1964 Alaskan earthquake and of its aftershock sequence, and these agree very well with the shallow angle thrust fault mechanism proposed by Plafker (1965). Both Plafker (1965, 1969) and Stauder & Bollinger (1966) agree that the dip of the fault surface associated with the 1964 Alaskan earthquake is extremely shallow, $\delta = 5° - 15°$. This shallow dip angle is supported also by the geographic distributions of aftershock activity following the 1964 Alaskan earthquake; the epicentral locations of the aftershocks are scattered over a rather broad zone (about 200 km wide by 600 km long) but all are associated with shallow hypocentres (depth h less than about 70 km). Focal mechanism studies of the 1960 Chilean earthquake are apparently a bit more ambiguous but on the whole are consistent with the model, deduced by Plafker & Savage (1970) from the local ground deformation data. There are some inconsistencies in the data, but the dip of the 1960 Chilean earthquake fault plane appears to be greater than that associated with the 1964 Alaskan earthquake. In general the nature of the faulting mechanism associated with both of these intensively studied earthquakes may be considered fairly well known. In this study the faulting associated with each of these earthquakes has been modelled by a point tangential displacement dislocation. The fault parameters h, θ_0, ϕ_0, α, δ, λ actually used in this study are listed in Table 1. Note that the dip δ of the 1964 Alaskan earthquake fault surface must be taken to be 170° (or equivalently $-10°$) in order to conform to the sign convention in Section 3; in the usual geological terminology, the dip is 10° in the direction N 65° W.

Table 1

Fault parameters used for numerical computation

Event	h (km)	θ_0	θ_0	α	δ	λ
1960 Chile	25	128·5°	285·5°	170°	35·5°	90°
1964 Alaska	50	28·0°	212·5°	155°	170°	270°

Measurements of local ground deformation are also useful in determining the slip-area $[A_0\,\overline{\Delta v}_0]$ associated with a particular earthquake. The slip-areas $[A_0\,\overline{\Delta v}_0]$ of both the 1960 Chilean earthquake and the 1964 Alaskan earthquake have been determined from local ground deformation data. The slip-area $[A_0\,\overline{\Delta v}_0]$ associated with both of these earthquakes is about $1{\cdot}2\times10^{12}\,m^3$. In the case of the Alaskan earthquake, this corresponds to a fault surface area A_0 about 600 km long by 200 km wide and a mean slip $\overline{\Delta v}_0$ of about 10 m (Plafker 1969). In the case of the Chilean earthquake, this corresponds to a fault surface area A_0 about 1000 km long by 60 km wide and a mean slip $\overline{\Delta v}_0$ of about 20 m. (Plafker & Savage 1970). In both cases the size of the fault surface area corresponds fairly well to the areal extent of the zone of major aftershock activity.

This value of the slip area for the 1964 Alaskan earthquake determined from local field observations agrees fairly well with the value $[A_0\,\overline{\Delta v}_0] = 2{\cdot}2\times10^{12}\,m^3$ obtained by Kanamori (1970) from a study of the excitation of long period seismic surface waves excited by that earthquake.

Given the fault parameters $h, \theta_0, \phi_0, \alpha, \delta, \lambda$ in Table 1 and the measured slip areas ($[A_0\,\overline{\Delta v}_0] = 1{\cdot}2\times10^{12}\,m^3$ for both earthquakes), one can use equation (50) to compute ΔC_{13} and ΔC_{23} produced by the Chilean and Alaskan earthquakes. The results are presented in Table 2. The Earth model used in computing ΔC_{13} and ΔC_{23} in Table 2 was SNREI Earth model 8073 AW. Also shown in Table 2 for comparison are the values of $|\Delta C| = (\Delta_{13}{}^2 + \Delta C_{23}{}^2)^{\frac{1}{2}}$ for the 1964 Alaskan earthquake as computed by Ben-Menahem & Israel (1970), using a homogeneous, non-gravitating Earth model, and by Mansinha & Smylie (1967), using a flat Earth model. Both Mansinha & Smylie (1967) and Ben-Menahem & Israel (1970) used a vertical dip slip fault as a model of the Alaskan earthquake faulting mechanism. Their results may however be compared with the results presented here since a vertical dip slip fault is dynamically equivalent to an horizontal dip slip fault (because of the symmetry of equation (37) in $\hat{\mathbf{n}}_0$ and $\hat{\mathbf{e}}_0$), and the actual Alaskan earthquake fault surface was nearly horizontal ($\delta = 10°$). It can be seen from Table 2 that the change $|\Delta C|$ in the inertia tensor which has been computed using SNREI Earth model 8073 AW is about ten times as great as the change $|\Delta C|$ computed by Ben-Menahem & Israel (1970) using a homogeneous Earth model.

The magnitude and direction of the net shift S_j of the mean pole of rotation by the Chilean and Alaskan earthquakes may be readily obtained from ΔC_{13j} and ΔC_{23j} in Table 2 by using equation (8). It was found that the theoretical angular

Table 2

Results of numerical computation compared with results for homogeneous non-gravitating Earth model (Ben-Menahem & Israel 1970) and mapped half-space model Mansinha & Smylie 1967)

Event	$(A_0\overline{\Delta v}_0)(m^3)$	ΔC_{13}(kg m^2)	ΔC_{23}	$\lvert\Delta C\rvert$	$\lvert\Delta C\rvert_{\text{homog}}$	$\lvert\Delta C\rvert_{\text{flat}}$
1960 Chile	$1{\cdot}2\times10^{12}$	$-1{\cdot}30\times10^{28}$	$-3{\cdot}44\times10^{28}$	$3{\cdot}68\times10^{28}$		
1964 Alaska	$1{\cdot}2\times10^{12}$	$-4{\cdot}95\times10^{27}$	$4{\cdot}84\times10^{28}$	$4{\cdot}86\times10^{28}$	$5{\cdot}03\times10^{27}$	$1{\cdot}92\times10^{27}$

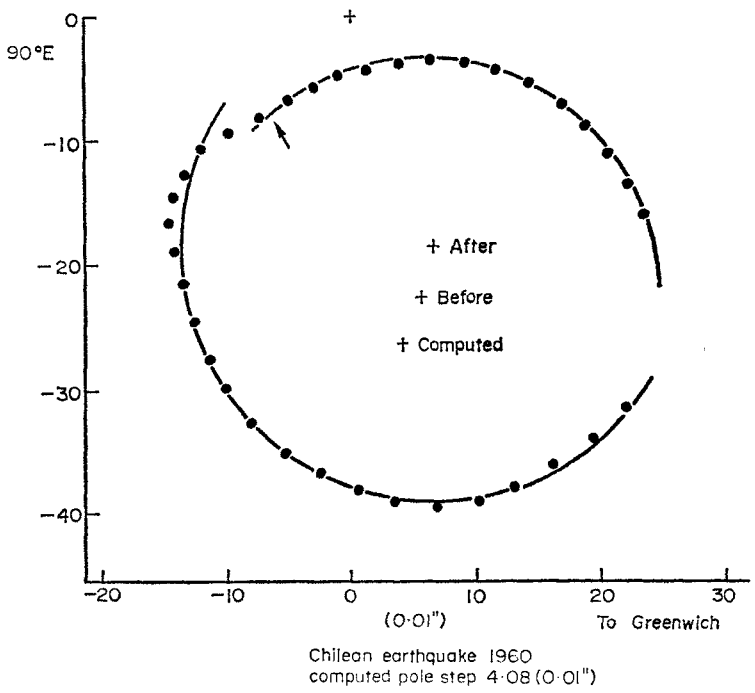

FIG. 7. Comparison of computed polar shift with polar shift inferred by Smylie & Mansinha (1968) from BIH polar motion data for the 1960 Chilean earthquake.

polar shift produced by the 1960 Chilean earthquake was 4·08 cs of arc (0·01 ″) in a direction toward western Canada (Vancouver Island). The theoretical angular polar shift produced by the 1964 Alaskan earthquake was 5·40 (0·01 ″) in a direction toward Siberia (Severnaya Zemlya).

These theoretically computed polar shifts S_j produced by the 1960 Chilean and 1964 Alaskan earthquakes can be compared with the observed polar shifts which Smylie & Mansinha (1968) determined by a process of searching for breaks in the astronomically observed polar motion data. The comparison is made in Figs 7 and 8 which are redrafted by eye from figures in Smylie & Mansinha (1968). The data points in Figs 7 and 8 are the measured positions of the Earth's rotation pole with respect to an $\hat{\mathbf{x}}_3$ axis taken through the Conventional International Origin, except that the apparent annual wobble component has been removed from each data point by Smylie & Mansinha (1968), using a standard harmonic analysis. The original polar motion data before removal of the annual component was that of the Bureau International de l'Heure (BIH). Each data point represents a 10-day average of independent polar motion data from several participating observatories. These measurements show a very poor agreement with the polar motion data collected by a separate organization, the International Polar Motion Service (IPMS). Smylie & Mansinha (1968) describe the process by which they have fitted circular arcs to the data points with the annual wobble component removed; the circular arcs which have been fitted to the data points for 1960 and for 1964 are shown in Figs 7 and 8. In Fig. 7 the time of occurrence of the 1960 Chilean earthquake is indicated by an arrow while in Fig. 8 the time of occurrence of the 1964 Alaskan earthquake is indicated by an arrow. The analysis procedure of Smylie and Mansinha does indicate that a break occurs in the Chandler wobble data both at the time of the 1960 Chilean earthquake and at the time of the 1964 Alaskan earthquake. According to their

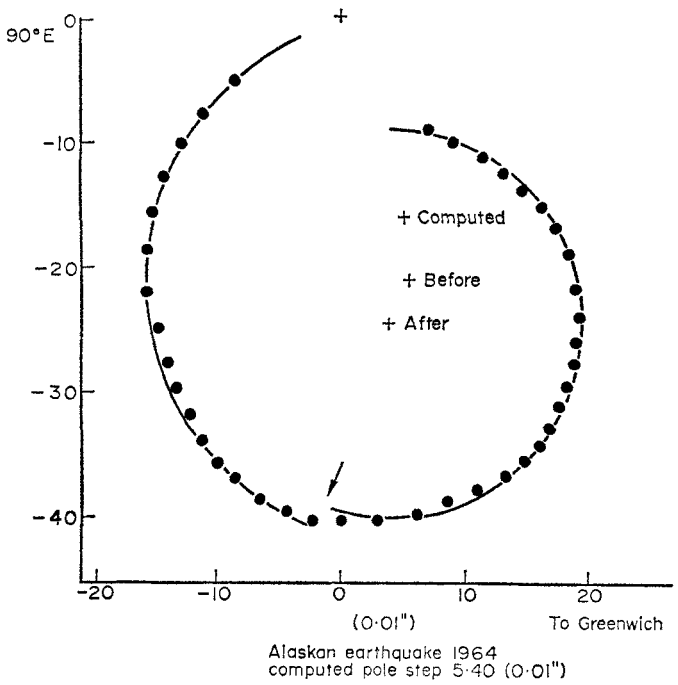

FIG. 8. Same as Fig. 7 for the 1964 Alsakan earthquake.

analysis, the mean pole of rotation in each case was shifted from the point labelled Before (the centre of the circular arc fitted to the data points before the time of the earthquake) to the point labelled After (the centre of the circular arc fitted to the data points after the time of the earthquake). In general the motion of the pole is counter-clockwise. Assuming that the position of the mean pole of rotation before the time of the earthquake was indeed at the point labelled Before, then in each case the theoretical polar shift computed here indicates that the mean pole should have been shifted in each case to the point labelled Computed. It can be seen from Figs 7 and 8 that for both the 1960 Chilean earthquake and the 1964 Alaskan earthquake, there is a complete lack of agreement between the computed theoretical polar shift and the polar shift obtained by the data analysis procedure of Smylie & Mansinha (1968). The reader might suspect from looking at Figs 7 and 8 that the disagreement is caused by a sign error in the theoretical computation, but in fact the computed direction of polar shift produced by both earthquakes may be verified by simple physical arguments. Provided that the faulting mechanism models are in both cases even reasonably realistic, it is in both cases the 'observed' polar shift and not the theoretical computed polar shift which is in the wrong direction.

In view of Haubrich's (1970) re-evaluation and criticism of the analysis procedure and results of Smylie & Mansinha (1968), it is not at all surprising that the theoretical computed polar shifts do not agree with their results. Haubrich (personal communication) has suggested that the noise level in the astronomical polar motion data is so severe that it might be impossible to observe directly the effect on the polar motion path of even the largest earthquake. The theoretical computations for the 1960 Chilean and 1964 Alaskan earthquakes certainly seem to support this hypothesis. These two earthquakes were the two largest earthquakes which occurred during the 11-year interval (1957–1967) for which Smylie & Mansinha (1968) conducted their polar motion data analysis. The theoretical polar shifts which would have been

produced by these two very large earthquakes were on the order of 4–5 (0·01″). The analysis of Smylie & Mansinha (1968) produced numerous breaks which were completely uncorrelated with any large ($M \geqslant 7{\cdot}5$) earthquake but which were associated with polar shifts several times as large as the largest theoretical polar shifts. The average size of all the polar shifts determined by Smylie & Mansinha (1968) was about 10 (0·01″) (Haubrich 1970), i.e. twice as large as the largest theoretical polar shifts. It thus appears that even the largest theoretical polar shifts are small compared to the noise level in the data of Smylie & Mansinha (1968). The complete lack of agreement between the theoretical computations and the data analysis of Smylie & Mansinha (1968) merely confirms the conclusions of Section 2 that a theoretical computation is necessary to test the hypothesis of Chandler wobble excitation by earthquakes.

The most likely explanation of the disagreement found above and of the other puzzling features of the analysis of Smylie & Mansinha (1968) which have been pointed out by Haubrich (1970) is that the polar motion data is contaminated by noise. Haubrich (1970 and personal communcation) presents other evidence completely unrelated to the data analysis procedure of Smylie & Mansinha (1968) which also suggests that the data is noisy outside the Chandler wobble frequency band. A high level of noise contamination is also suggested by the very poor agreement between the raw polar motion data of the BIH and that of the IPMS. The data definitely does suffer from noise contamination and it is likely that no data analysis procedure would allow one to detect the excitation process. However, there does seem to me to be a conceptual mistake in the procedure by which both Smylie & Mansinha (1968) and Haubrich (1970) searched for a correlation with earthquakes. If the data were re-analysed with this mistake rectified, then perhaps at least the effect on the polar motion path of the largest earthquakes (e.g. the Chilean and Alaskan earthquakes) could be detected, and the agreement with the theoretical computations might be improved.

The conceptual mistake lies in the fact that both investigators attempted to fit the data points between the times of occurrence of earthquakes by circular arcs. In doing so, they have of course assumed that the only significant changes with time in the inertia tensor components $C_{13}(t)$ and $C_{23}(t)$ were the sudden changes ΔC_{13j} and ΔC_{23j} which occurred at the times t_j of the earthquakes. An earthquake however represents a sudden release (through some type of failure) of an elastic strain field which had slowly accumulated within the Earth before the time of the earthquake. Tectonic processes within the Earth are presumably always acting to slowly build up elastic strain energy within the Earth, and these tectonic elastic strains are being continually released by the occurrence of earthquakes in the Earth's lithosphere. On the average over a long period of time, earthquakes act to release all the elastic strain energy which would otherwise have been stored up within the Earth. The elastic strain fields which are building up slowly within the Earth between the times of occurrence of earthquakes give rise to associated slow changes $C_{13}(t)$ and $C_{23}(t)$ in the inertia tensor components of the Earth. The position of the Earth's mean pole of rotation between the times of earthquakes will thus not remain fixed, but will rather follow the slow elastic changes in the axis of figure due to the slow building up of elastic strains. No Chandler wobble will be excited by these very long period (compared to 14 months) changes. If the material comprising the Earth behaved perfectly elastically to the application of slowly changing tectonic forces (except for the sudden localized material failures associated with earthquake faulting), then on the average over a long period of time the mean pole of rotation would migrate slowly between the times of earthquakes at a rate equal to the root mean square polar shift per unit time due to earthquakes, $\langle R^2 \rangle^{\frac{1}{2}}$. Since earthquakes would act to relieve the buildup of elastic strain energy, there could be no large-scale polar wandering on the average over long periods of time. Of course the material com-

prising the Earth does not behave perfectly elastically over long periods of time and this conclusion about the rate of slow polar wandering neglects the fact that there are also anelastic processes within the Earth (e.g. thermal convection in the Earth's mantle, post-glacial isostatic uplift of Fennoscandia and the Canadian shield, etc.) which will also give rise to slow changes in the mean pole of rotation (Goldreich & Toomre 1969). In any case the data analysis procedure of Smylie & Mansinha (1968) is invalid because they have completely neglected the slow migration of the mean pole of rotation in response both to slow elastic and to slow anelastic redistributions of the Earth's mass. Earthquakes cannot by themselves give rise to polar wandering, but the data analysis procedure of Smylie & Mansinha (1968) implicitly assumes that they can. Neglect of the slow migration of the mean pole of rotation between the times of occurrence of earthquakes could significantly affect the results of the analysis. This question is presently being pursued and the results will be reported in the future. Hopefully the noise level in the BIH polar motion data is not so high that at least the effects of the Chilean and Alaskan earthquakes can be detected and compared with the theoretical computations reported here.

5. Theoretical Chandler power

The total theoretical Chandler wobble power produced by a series of N earthquakes occurring during a time interval T_N is given by equation (14)

$$P = \frac{Q}{\omega_0} \langle R^2 \rangle \tag{51}$$

where ω_0 is the angular frequency of oscillation and where $\tau = 2Q/\omega_0$ is the decay time of the Chandler Wobble. The expression

$$\langle R^2 \rangle = \frac{1}{T_N} \left| \sum_j^N S_j \exp(-i\omega_0 t_j) \right|^2$$

is the mean square polar shift per unit time due to the series of sudden mass redistributions associated with the earthquake sequence.

The actual Chandler wobble power, as well as the free angular frequency ω_0 and Q (or decay time τ) appearing in (51) may be determined from an analysis of the astronomical observation of the motion of the Earth's pole of rotation. Several investigators have conducted analyses of the polar motion data of the International Latitude Service. Table 3 is a summary of some of these recent determinations of Chandler power P, Chandler period $T_0 = 2\pi/\omega_0$, and Chandler Q. It can be seen from Table 3 that the free period T_0 of the Chandler wobble is fairly well determined; the mean of all the observations is about 1·18 years. The total observed Chandler

Table 3

Summary of recent determinations of Chandler wobble parameters

Investigator	T_0 (years)	Chandler power P $(0{\cdot}01'')^2$	Q
Rudnick 1956	1·193	96	30
Walker & Young 1957	1·193		30–100
Munk & MacDonald 1960	1·183	143	30
	1·178	196	60
Fellgett 1960	1·180	259	33
Jeffreys 1968	1·186		62
Haubrich & Munk 1959 (pole tide)			100–200

wobble power P has not been so accurately determined, but it is on the order of 200 $(0{\cdot}01\,'')^2$. The root mean square angular deviation of the instantaneous axis of rotation from the reference axis $\hat{\mathbf{x}}_3$ is thus about 14 to 15 cs of arc $(0{\cdot}01\,'')$.

The parameter which is most uncertain is the Q of the Chandler wobble. The Q or decay time τ is extremely difficult to estimate from the astronomical polar motion data because of the continual re-excitation of the wobble by the excitation mechanism. The two most recent and probably best investigations of the International Latitude Service polar motion data are those of Fellgett (unpublished work, 1960; result listed in footnote p. 174 of Munk & MacDonald 1960) and Jeffreys (1968). Both Fellgett and Jeffreys used a maximum likelihood method of estimation to determine the Chandler wobble parameters ω_0, P, and Q. Both investigations revealed that the data appeared to be fit best by a rather low value of Q, but that the uncertainty in the estimate was quite high. Furthermore both Fellgett (1970, personal communication) and Jeffreys (1970, personal communication) comment on the fact that the probability distribution associated with the estimation of Q is far from normal; the uncertainties are such that the actual Q cannot be much lower than the values listed in Table 3 but could easily be several times higher. A Chandler wobble Q as high as 100–200 appears to be readily compatible with the present astronomical polar motion data.

The final Q determination in Table 3 (Haubrich & Munk 1959) was not made by analysing astronomical data but was rather made by analysing observations of the pole tide. The pole tide is a tidal motion of the Earth's oceans with a typical surface vertical displacement amplitude of 0·5 cm and a period of 14 months. This motion of the Earth's oceans is driven by the 14 month free Chandler wobble of the Earth's pole of rotation. Haubrich & Munk (1959) analysed oceanic tidal records from various tidal stations in order to detect the pole tide; their analysis indicated a Chandler wobble $Q > 100$, but due to the extremely low signal to noise ratio in the pole tide spectra this evidence must be considered somewhat marginal.

The quality of the present Chandler wobble data does not then even allow a reasonably accurate measure of the Q of the Chandler wobble. The Q is uncertain by about a factor of ten; it can be as low as 20–30 or as high as 200–250.

This extreme uncertainty in the value of the Q of the Chandler wobble makes it difficult to identify the mechanism of the Chandler wobble energy dissipation. For example, if the Q really is as high as 200, then it is extremely reasonable to attribute all the damping to elastic afterworking in the mantle, the same process by which the higher frequency gravitational-elastic normal modes are damped. If, however, the Q is really 20–30 then some mechanism other than elastic shear energy dissipation in the mantle must be acting to damp the Chandler wobble. The large uncertainty in Q will also of course hinder the attempt to test the hypothesis that earthquakes are responsible for the generation and maintenance of the Chandler wobble, since the theoretical Chandler power P in (51) produced by an earthquake sequence is proportional to Q.

It is instructive at this point to consider a simple hypothetical example of the use of (51) to test the hypothesis that earthquakes are responsible for the generation of the Earth's Chandler wobble. It was shown in Section 4 that the theoretical magnitude of the polar shift caused by the 1964 Alaskan earthquake was 5·40 $(0{\cdot}01\,'')$. Consider a model Earth on which the only seismic activity consists of one 1964 Alaskan type type earthquake per year. In that case $\langle R^2 \rangle$, the mean square pole shift per year due to earthquake events, could be as high as $(5{\cdot}40)^2$ $(0{\cdot}01\,'')^2$/yr, or about 30 $(0{\cdot}01\,'')^2$/yr. The resulting Chandler wobble power produced on such an Earth model is shown in Table 4 for various values of the Chandler wobble Q. If the Q were as low as 30, then the effect of one 1964 Alaskan type earthquake per year would almost be sufficient to maintain the Earth's observed Chandler wobble activity of about 200 $(0{\cdot}01\,'')^2$. If the Q were as high as 200, then one 1964 Alaskan type

Table 3

Chandler wobble power produced by one 1964 *Alaskan earthquake per year*

Q	Chandler power P $(0{\cdot}01'')^2$
30	165
100	550
200	1100

earthquake every 5–6 years would be all that was required. This hypothetical example helps to give one a feeling for the amount of seismic activity which is necessary to maintain the Earth's observed Chandler wobble activity. In order to really test the hypothesis, one would like to obtain an accurate estimate of $\langle R^2 \rangle$ from the real sequence of past earthquakes which have been recorded on the Earth since around the turn of the century. It will be seen that a really accurate estimate of $\langle R^2 \rangle$ cannot be obtained from the existing data in the seismic catalogue.

The theory of Section 3, particularly equation (50) can theoretically be used to estimate $\langle R^2 \rangle$, the mean square pole shift per unit time due to any sequence of earthquake events. In order to use (50) to compute the pole shift

$$S_j = \left(\frac{\Omega}{\omega_0}\right) \frac{\Delta C_j}{A} \tag{53}$$

associated with the jth earthquake in the sequence, one must be able to specify the slip-area $[A_0\, \overline{\Delta v}_0]$ as well as the location and geometry $h, \theta_0, \phi_0, \alpha, \delta, \lambda$ of the faulting associated with the jth earthquake. Unfortunately, there are very few past earthquakes (the 1960 Chilean earthquake and 1964 Alaskan earthquake are two) for which reliable determinations of these various quantities exist. For most past large earthquakes, the only information which is readily available is that listed in the standard seismic catalogues (Gutenberg & Richter 1954; Richter 1958; Duda 1965). The data listed are the date and time of occurrence t_j, epicentral coordinates θ_0, ϕ_0 and depth h, and the magnitude, either the body wave magnitude m or the surface wave magnitude M (Richter 1958). These are the only parameters which have been measured and recorded for the majority of past large earthquakes; a few past large earthquakes have however been studied in greater detail.

For some past earthquakes, P-wave first motion studies have been used to deduce the geometry of the focal mechanism. A well constrained first motion focal mechanism solution allows one to determine the orientation of the fault plane and of the slip vector $(\alpha, \delta, \lambda)$. (Actually there is an ambiguity in the determination of the fault plane and the auxiliary plane which can usually be resolved using geological evidence but which is irrelevant in this study since the same ambiguity occurs in equation (37) also). McKenzie & Parker (1967) have shown that first motion fault mechanism solutions for earthquakes around the North Pacific agree remarkably well with the hypothesis of rigid lithospheric plate tectonics (Isacks *et al.* 1968). In view of this fact, it is probable that a reasonable guess can be made as to the faulting mechanism responsible for most past shallow focus (say $h \leqslant 60$ km) earthquakes by assuming that they occur in accordance with the present relative lithospheric plate motions. Thus any shallow focus earthquake located on an oceanic transform fault presumably has a strike-slip mechanism whereas any shallow focus earthquake located in an island arc or oceanic trench zone presumably represents underthrusting of one plate under another and has a shallow angle thrust mechanism. Both the fault strike azimuth (Morgan 1968) and the horizontal projection of the slip vector (McKenzie & Parker 1967) for any such shallow earthquake can be deduced from a knowledge of the relative plate motions (Le Pichon 1968). Unfortunately there are some shallow

focus earthquakes, notably in central Asia, which do not occur on any readily defined plate boundary, and for these earthquakes it is difficult to make a reasonable guess as to the mechanism. Furthermore, it is only possible to use the plate tectonic theory to infer the faulting mechanism of shallow focus earthquakes; deep focus earthquake mechanisms cannot be deduced from a knowledge of relative lithospheric plate motions. Fault mechanism solutions which have been obtained for deep focus earthquakes located in the deep Benioff zones behind island arcs and oceanic trenches seem to indicate that the mechanisms are not indicative of simple underthrusting (Isacks *et al.* 1968). The plate tectonic hypothesis could then allow one to make a reasonable guess as to the fault geometry parameters α, δ, λ of many large shallow focus earthquakes, but one cannot in this way infer α, δ, λ for all past large earthquakes.

The slip-area $[A_0\,\overline{\Delta v}_0]$ is another quantity which is difficult to infer for an individual earthquake from the information listed in the standard seismic catalogues. The most reliable and accurate method of determining the fault plane area A_0 and the net slip $\overline{\Delta v}_0$ associated with an earthquake is probably to utilize field observations of ground deformation in the earthquake vicinity. Unfortunately there are very few earthquakes for which even relatively complete observations of local ground deformation have been collected. The 1960 Chilean earthquake and the 1964 Alaskan earthquake seem to be the only two recent very large earthquakes which have been intensively studied in this respect.

It is also possible to use seismic methods, i.e. analysis of seismograms recorded at teleseismic distances, to estimate the slip-area $[A_0\,\overline{\Delta v}_0]$ associated with an earthquake Note first that the slip-area $[A_0\,\overline{\Delta v}_0]$ of an earthquake is closely related to the more widely used earthquake moment M_0. The moment M_0 of an earthquake fault has been defined and used in various contexts in the past (Maruyama 1963; Burridge & Knopoff 1964; Aki 1966; Brune & Allen 1967; Brune 1968; Davies & Brune 1971). If μ is the rigidity of the material in the earthquake zone, then M_0 is defined as

$$M_0 = \mu[A_0\,\overline{\Delta v}_0]. \tag{54}$$

The quantity which is listed in the standard seismic catalogues as an indication of the size of the various earthquakes is of course not the moment M_0 but the earthquake magnitude M. The surface wave magnitude M of an earthquake is determined in terms of the amplitude of the associated seismic surface waves with a period of 20 s (Gutenberg & Richter 1954). It can be shown (Ben-Menahem & Harkrider 1964; Burridge & Knopoff 1964) that the amplitude of seismic surface waves excited by a point tangential displacement dislocation in a stratified elastic half-space is proportional to the slip-area $[A_0\,\overline{\Delta v}_0]$ or the moment M_0 of the source, provided that the wavelength and period of the seismic waves are long compared with the source dimensions and time. For larger earthquakes with larger fault dimensions, Brune & King (1967) have shown that the use of 20-s surface waves does not provide a reliable estimate of the slip area. It is necessary to measure the spectral amplitudes of lower frequency seismic surface waves excited by a large earthquake if one wishes to obtain an accurate determination of the slip-area by using seismic methods. Brune & King (1967) and Brune & Engen (1969) have analysed 100-s Rayleigh and Love surface waves excited by a few large past earthquakes in order to obtain more accurate estimates of the associated earthquake moments M_0. The analyses of 21 selected past earthquakes are summarized by Brune & Engen (1969), who have chosen to present their results in the form of a newly-defined 100-s surface wave earthquake magnitude or mantle wave magnitude M_m. For some of the 21 earthquakes studied the 100-s mantle wave magnitude M_m differed from the usual 20-s surface wave magnitude by 0·5 (e.g. for the 1964 Alaskan earthquake $M = 8{\cdot}4$, $M_m = 8{\cdot}9$ but for the 1933 Sanriku, Japan earthquake $M = 8{\cdot}9$, $M_m = 8{\cdot}4$). Other investigators have analyzed even longer period Love and Rayleigh surface waves excited by large past earthquakes in order to determine seismic moments M_0. For example Kanamori

(1970 a, b, and personal communication) has used seismic evidence from 100–400-s surface waves to determine the seismic moment of the 1963 13 October Kurile earthquake, the 1964 Alaskan earthquake, the 1965 February 4 Rat Island earthquake, and the 1968 May 16 Tokachi-Oki earthquake. Brune & Jarosch (1970, personal communication) have recently undertaken a large-scale project designed to determine the seismic moments of as many large past earthquakes as possible. Until, however, such

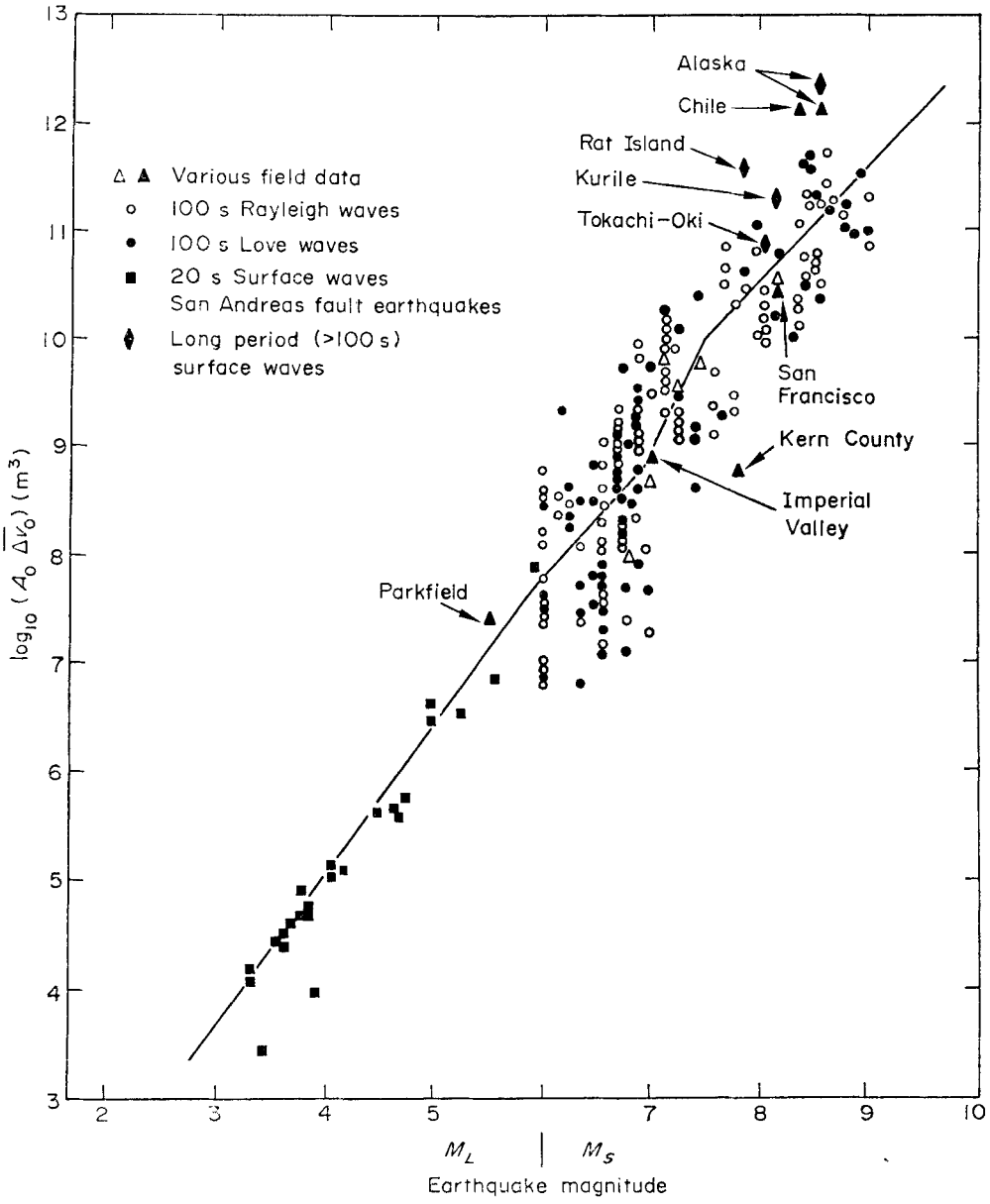

FIG. 9. Plot showing moment–magnitude relation of Brune (1968) and Wyss & & Brune (1968) converted to a slip-area ($A_0\,\overline{\Delta v_0}$) vs. magnitude relationship. Redrafted somewhat schematically from figures in Brune & King (1967), Brune (1968), Wyss & Brune (1968) and Brune & Engen (1969). Also shown are some seismic slip areas for recent earthquakes determined by Kanamori (1970 and personal communication).

a project has actually been completed, one must rely on cruder estimates of the moments M_0 or the slip-areas $[A_0\,\overline{\Delta v}_0]$ associated with the vast majority of large past earthquakes.

Brune (1968) has developed an empirical relation which can be used to infer a crude estimate of the moment M_0 of a large earthquake if only its 20-s surface wave magnitude M is known. This empirical relation has been refined by Wyss & Brune (1968) for application to smaller earthquakes in localized regions of seismic activity. The relation for strike slip earthquakes is depicted in Fig. 9 as a relation between slip-area $[A_0\,\overline{v\Delta}_0]$ and magnitude M. The relation shown in Fig. 9 was derived from the relation of Brune (1968) and Wyss & Brune (1968) by using the value $\mu = 3{\cdot}3\times 10^{11}$ dyne cm^{-2} in equation (54) defining moment in terms of slip-area. For earthquakes with $M \leqslant 7{\cdot}0$, the relation depicted in Fig. 9 may be written algebraically as

$$\log_{10}[A_0\,\overline{\Delta v}_0] = 2{\cdot}5+M, \qquad M \geqslant 7{\cdot}5$$

$$\log_{10}[A_0\,\overline{\Delta v}_0] = 7{\cdot}3+2{\cdot}3M, \quad 7{\cdot}0 \leqslant M \leqslant 7{\cdot}5 \tag{55}$$

where the slip area $[A_0\,\overline{\Delta v}_0]$ is expressed in m.k.s. units of m^3. For dip slip earthquakes, the slip-area $[A_0\,\overline{\Delta v}_0]$ obtained from the relation given in (55) and depicted in Fig. 9 should be multiplied by a factor of 2·5 (Brune & Engen 1969). This extra factor of 2·5 recommended by Brune & Engen (1969) is an attempt to take account of the fact that dip-slip earthquakes are less efficient generators of seismic surface waves at all frequencies.

The various points in Fig. 9 represent independent determinations of the moments M_0 of a few selected earthquakes by various techniques. The triangles represent earthquake moments deduced from field observations of local ground deformation associated with the earthquakes. All except the points for the 1960 Chilean earthquake (Plafker & Savage 1970) and the 1964 Alaskan earthquake (Plafker 1969) are taken from Brune & Allen (1967). It is the opinion of the author that except for 1960 Chile, 1964 Alaska, and a few California strike slip earthquakes (the shaded triangles in Fig. 9), the earthquake moments M_0 determined from field observations are in many cases little more than a guess. The circles in Fig. 9 represent seismic moments M_0 determined by Brune & King (1967) and Brune & Engen (1969) by analysing 100-s Love and Rayleigh waves (actually the 100-s Rayleigh wave points are merely properly scaled 100-s surface wave amplitudes measured at an individual station; this certainly accounts for some of the scatter). The diamonds in Fig. 9 represent seismic moment determinations from longer period surface wave studies by Kanamori (1970, and personal communication). The squares in Fig. 9 represent moment determinations for small earthquakes (local magnitude $M_L \leqslant 6{\cdot}0$) on the San Andreas Fault. The moments for these small earthquakes have been determined by Wyss & Brune (1968) using 20-s surface waves; below $M = 6{\cdot}0$, the local magnitude scale M_L (Gutenberg & Richter 1954; Wyss & Brune 1968) is used in assigning magnitudes. It is clear from the work of Wyss & Brune (1968) and from Fig. 9 that a regional moment-local magnitude relation (such as that in Fig. 9 for the San Andreas fault) may be used with some confidence to infer reasonably accurate earthquake moments M_0 from assigned local magnitudes M_L. It is also clear from Fig. 9 that for the larger earthquakes, the use of the simple empirical relation (55) to estimate individual earthquake moments may lead to rather substantial errors. Brune (1968) estimates that the assignment of the moment M_0 to a particular earthquake on the basis of magnitude alone may be uncertain by more than a factor of 5. Two possibly extreme examples are shown in Table 5, the 1960 Chilean earthquake ($M = 8{\cdot}3$, $M_m = 8{\cdot}8$) and the 1964 Alaskan earthquake ($M = 8{\cdot}4$, $M_m = 8{\cdot}9$). For both of these earthquakes, the slip-area $(A_0\,\overline{\Delta v}_0]$ deduced from M using (55) is too low by a factor of almost 10 compared to the slip-area $[A_0\,\overline{\Delta v}_0]$ deduced from field evidence. In fact even the slip areas $[A_0\,\overline{\Delta v}_0]$ determined from the analyses of the excited 100-s Love

Table 5

Summary of various estimations of slip-areas ($A_0\,\overline{\Delta v}_0$) *for* 1960 *Chilean and* 1964 *Alaskan earthquake*

Event	M	M_m	$(A_0\,\overline{\Delta v}_0)$ $= 2{\cdot}5(10^{2{\cdot}5+M})$	$(A_0\,\overline{\Delta v}_0)$ $= 2{\cdot}5(10^{2{\cdot}5+Mm})$	$(A_0\,\overline{\Delta v}_0)$ (Field)	$(A_0\,\overline{\Delta v}_0)$ (Kanamori)
1960 Chile	8·8	8·8	$1{\cdot}6\times10^{11}$	$5{\cdot}0\times10^{11}$	$1{\cdot}2\times10^{12}$	
1964 Alaska	8·4	8·9	$2{\cdot}0\times10^{11}$	$6{\cdot}2\times10^{11}$	$1{\cdot}2\times10^{12}$	$2{\cdot}2\times10^{12}$

and Rayleigh waves (i.e. computed using the 100-s mantle wave magnitudes M_m in (55)) are too low by a factor of 2–3.

Use of the slip-area vs. 20-s surface wave magnitude relation (55) can lead to large errors or uncertainties in the assignment of a slip-area to an individual earthquake. Unless however there is some systematic error in the relation (55), use of the relation should provide a fairly good estimate of the net slip-area accumulation due to a sequence of past earthquakes in the seismic catalogue, since the individual errors should average out. Davies & Brune (1971) have utilized the moment-magnitude relation of Brune (1968) to compute rates of fault slip due to earthquakes located on various lithospheric plate boundaries. They find that the rates of fault slip at various boundaries computed from the net seismicity agree well with the rates of relative plate motion obtained from other methods, notably analysis of ocean floor magnetic anomaly patterns (Le Pichon 1968). This good agreement suggests that the seismic moment–magnitude relation is reasonably accurate in an average sense, i.e. that it will provide a reasonably accurate estimate of the net moment accumulation or slip-area release due to a series of past earthquakes. This work of Davies & Brune (1971) and its bearing on the possibility of a systematic error in the seismic moment–magnitude relation will be discussed in more detail later.

There is thus a complete lack of even inferred information about the fault parameters α, δ, λ associated with many past earthquakes (e.g. deep focus earthquakes). There is also a large uncertainty (by more than a factor of 5) in the estimation of the slip-area $[A_0\,\overline{\Delta v}_0]$ associated with almost all past earthquakes. In view of these uncertainties, it would be impossible to try to actually compute the magnitude and direction of the pole shift S_j produced by every past large earthquake which is listed in the standard seismic catalogues. In this study a much cruder method has been used to estimate $\langle R^2\rangle$, the mean square pole shift due to past large earthquakes.

The catalogue of past seismic events used in this study to estimate $\langle R^2\rangle$ is that of Duda (1965). This is a list of earthquakes of magnitude $M \geqslant 7{\cdot}0$ which is thought to be complete or almost complete for the 61-year span 1904–1964. The catalogue of Duda (1965) is identical to that of Gutenberg & Richter (1954) with revised magnitudes by Richter (1958) and with the addition of a few smaller earthquakes detected by Duda for the period 1904–1917. There were 1201 earthquakes of magnitude $M \geqslant 7{\cdot}0$ during the 61 years 1904–1964.

For the purposes of this study, each of these 1201 earthquakes was classified as being one of three types: type 1— shallow focus strike-slip mechanism, type 2— shallow focus shallow angle dip-slip mechanism, type 3—deep focus. The classification of a particular earthquake was made purely on the basis of its location as given by Duda (1965). Any earthquake with a depth of focus $h \geqslant 100$ km was classified type 3. If a shallow focus ($h \leqslant 100$ km) earthquake occurred in an island arc or oceanic trench zone or in a continental compressive tectonic zone (e.g. Iran, the Himalayas), then it was classified type 2. If a shallow focus ($h \leqslant 100$ km) earthquake occurred on an oceanic transform fault or on a continental transform or or transcurrent fault (e.g. the San Andreas fault), then it was classified type 1.

The map in McKenzie (1969) showing the approximate position and nature of the major lithospheric plate boundaries was used as a guide in making this earthquake classification. There were of course a few shallow earthquakes which were difficult to classify easily in this way, but every earthquake in the list was given a classification. This simple classification scheme indicated that about 70 per cent of the Earth's large ($M \geqslant 7{\cdot}0$) earthquakes have a shallow angle thrust fault mechanism (type 2); about 10 per cent were shallow strike slip earthquakes (type 1) and about 20 per cent were deep focus earthquakes (type 3).

Recall that the changes in the inertia tensor components ΔC_{13} and ΔC_{23} produced by an individual earthquake can be written in the form

$$\begin{aligned} \Delta C_{13} &= [A_0\,\overline{\Delta v}_0]\, g_{13}(h, \theta_0, \phi_0, \alpha, \delta, \lambda) \\ \Delta C_{23} &= [A_0\,\overline{\Delta v}_0]\, g_{23}(h, \theta_0, \phi_0, \alpha, \delta, \lambda) \end{aligned} \tag{56}$$

where the factors $g_{13}(h, \theta_0, \phi_0, \alpha, \delta, \lambda)$ and $g_{23}(h, \theta_0, \phi_0, \alpha, \delta, \lambda)$ depending on the location and geometry of the associated earthquake fault are written out explicitly in equations (50). Three different kinds of average values of the quantity $g = (g_{13}{}^3 + g_{23}{}^2)^{\frac{1}{2}}$ were computed using (50), one average value for each of the three types of earthquakes used in the classification scheme. First note that $g = (g_{13}{}^2 + g_{23}{}^2)^{\frac{1}{2}}$ is independent of the longitude ϕ_0 of the fault location. The first average $\langle g_1 \rangle$ was computed for vertical strike slip faults ($\delta = 90°$, $\lambda = 0°$) averaged over all possible values of strike azimuth $0° \leqslant \alpha \leqslant 180°$, colatitude $0° \leqslant \theta_0 \leqslant 180°$, and depth $0 \leqslant h \leqslant 20$ km. The sort of variation in g with respect to α and θ_0 which is being averaged out may be seen in Fig. 5. The second average $\langle g_2 \rangle$ was computed for shallow angle dip slip faults ($\lambda = 90°$) averaged over fault dip angles $10° \leqslant \delta \leqslant 45°$ and over all possible values of strike azimuth $0° \leqslant \alpha \leqslant 180°$, colatitude $0° \leqslant \theta_0 \leqslant 180°$, and depth $0 \leqslant h \leqslant 60$ km. In this case the sort of variation in g with respect to α and θ_0 which is being averaged out may be seen in Fig. 6. The third average $\langle g_3 \rangle$ was taken over all possible fault locations θ_0 and orientations α, δ, λ and for all deep focus depths $100 \leqslant h \leqslant 700$ km. Thus $\langle g_1 \rangle$ is a measure of the average effect of an earthquake of type 1. $\langle g_2 \rangle$ is a measure of the average effect of an earthquake of type 2, and $\langle g_3 \rangle$ is a measure of the average effect of an earthquake of type 3. The averages obtained using equation (50) for SNREI Earth model 8073 AW were $\langle g_1 \rangle = 0{\cdot}417 \times 10^{17}$, $\langle g_2 \rangle = 0{\cdot}290 \times 10^{17}$, $\langle g_3 \rangle = 0{\cdot}310 \times 10^{17}$ in mks units (i.e. if $[A_0\,\overline{\Delta v}_0]$ is given in m^3, then $\Delta C = [A_0\,\overline{\Delta v}_0] \times \langle g \rangle$ is in kg m^2). Thus on the average a shallow strike slip earthquake produces a larger polar shift than a shallow angle dip slip earthquake having the same slip-area $[A_0\,\overline{\Delta v}_0]$.

For almost all of the 1201 earthquakes used, the slip-area $[A_0\,\overline{\Delta v}_0]$ was inferred from the relation (55), using the earthquake magnitude M given by Duda (1965) and remembering to multiply the resulting slip-area by a factor of 2·5 (Brune & Engen 1969) for the earthquakes of type 2. For the 21 earthquakes assigned mantle wave magnitudes M_m by Brune & Engen (1969), M_m was used in (55) to infer the slip-area; for the 1963 Kurile earthquake, the slip-area was taken from Kanamori (1970). The slip-areas $[A_0\,\overline{\Delta v}_0]$ of both the 1960 Chilean earthquake and the 1964 Alaskan earthquake were taken as $1{\cdot}2 \times 10^{12}$ m^3 on the basis of field observation of local ground deformation (see Section 3). Fig. 10 is a plot showing the net slip-area release on earthquake faults during each year in the span 1904–1964; the slip-area of each earthquake in the list of Duda (1965) was inferred as described above. It may be seen from Fig. 10 that the years 1905–1906 were years of comparatively intense seismic activity. It also appears from the plot that both 1960 and 1964 were years of comparatively high activity but this feature is due entirely to the fact that the slip-areas of the 1960 Chilean earthquake and the 1964 Alaskan earthquake used in this study were several times higher than the slip-area inferred for any other earthquake

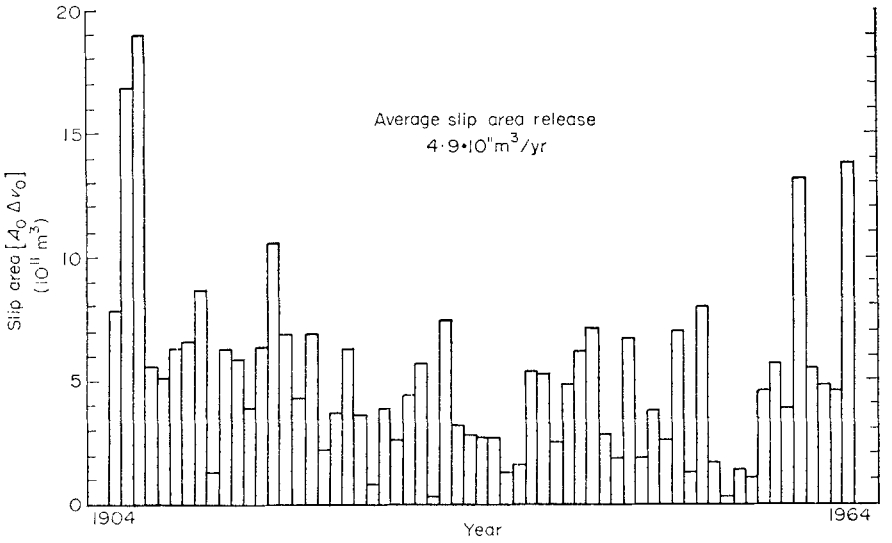

FIG. 10 Graph of slip-area release per year for the period 1904–1964.

included in the study. Brune (1968) has pointed out that in a study of this kind, the very few extremely large earthquakes in any sequence account for most of the slip-area accumulation. The average slip-area release per year of all earthquakes of magnitude $M \geqslant 7{\cdot}0$ occurring in the time span 1904–1964 is $4{\cdot}9 \times 10^{11}$ m^3/yr, which corresponds to one earthquake the size of the 1964 Alaskan earthquake about every 2–3 years.

A simple Monte Carlo technique was used to estimate $\langle R^2 \rangle$. It was assumed that each earthquake in the sequence listed by Duda (1965) produced a pole shift of magnitude $|S_j|$ given by either $[A_0\,\overline{\Delta v}_0]\langle g_1 \rangle$, $[A_0\,\overline{\Delta v}_0]\langle g_2 \rangle$, or $[A_0\,\overline{\Delta v}_0]\langle g_3 \rangle$, depending on whether the earthquake was classified type 1, type 2, or type 3 (except for the 1960 Chilean earthquake and the 1964 Alaskan earthquake, for which the true values $|S_j|$ given in Section 3 were used). The phase factors $\exp(-i\omega_0 t_j)$ have the effect of completely randomizing the total phase of each term in the sum (52). Thus $\langle R^2 \rangle$ may be estimated by assuming that it represents the outcome of a two-dimensional random walk process with step sizes $|S_j|$ and with each step in a random direction. It is hoped that the errors which arise in estimating the pole shifts $|S_j|$ in the simple way used here will be averaged out in the estimation of the net mean square pole shift in 61 years. Five hundred simulated two-dimensional random walks were made on a computer using as step sizes the 1201 pole shifts $|S_j|$ computed as described above. This Monte Carlo experiment yields a mean square pole shift per year produced by the 1201 earthquakes of magnitude $M \geqslant 7{\cdot}0$ in the period 1904–1964 of

$$\langle R^2 \rangle = 1{\cdot}1 \quad (0{\cdot}01\,'')^2/\text{yr}. \tag{57}$$

This corresponds to a mean square pole shift per year equivalent to that which would be produced by one 1964 Alaskan-sized earthquake about every 25–30 years. Recall that the net slip-area release corresponds to one 1964 Alaskan-sized earthquake about every 3 years. The reason for this difference is that in any two-dimensional random walk process it is really only the few largest steps in the process which greatly affect the outcome.

The total Chandler wobble power P produced by an excitation process with a mean square pole shift per year of $\langle R^2 \rangle = 1{\cdot}1(0{\cdot}01\,'')^2/\text{yr}$ is shown in Table 6 for

Table 6

Chandler power P produced by earthquakes estimated using moment–magnitude relation of Brune (1968) *compared with atmospheric excitation measured by Munk & Hassan* (1961)

Q	Chandler power P $(0{\cdot}01'')^2$	Atmospheric
30	6·6	2·5
100	21·8	8·3
200	43·6	16·6

various values of the Chandler wobble Q. Also shown in Table 6 for comparison is the Chandler wobble power which is produced by motions of the Earth's atmosphere with a 14-month period, as measured by Munk & Hassan (1961). The computed theoretical Chandler power P produced by earthquakes is seen to be about three times as great as that generated by atmospheric motions, but it is disappointingly low compared to the observed level of Chandler wobble activity of about 200 $(0{\cdot}01'')^2$.

There are however several reasons why the actual Chandler wobble power produced by earthquakes and earthquake-associated processes in the Earth's crust and upper mantle is probably larger than this computation seems to indicate.

The major uncertainty in the computation is in the assignment of slip-areas $[A_0\,\overline{\Delta v}_0]$ to individual earthquakes through the use of the seismic moment-magnitude relation of Brune (1968). The theoretical Chandler power P in equation (51) produced by a sequence of earthquakes depends on the squares of the slip-areas $[A_0\,\overline{\Delta v}_0]$ of the earthquakes in the sequence. The outcome of the calculation done here thus depends critically on the most uncertain factor in the whole calculation. There are several considerations which suggest that in general the earthquake slip-areas used in the evaluation of (52) should in fact be increased over the values which were actually used.

The moment–magnitude relation of Brune (1968) was developed on the basis of a study of the excitation of 100 second Love and Rayleigh waves. Aki (1967, and personal communication 1970) has suggested on the basis of his scaling law of the seismic spectrum, that for very large earthquakes (say $M \geqslant 8{\cdot}0$), it is necessary to examine longer period surface waves in order to obtain an accurate estimate of the seismic moment M_0. The ω^2 earthquake spectral model proposed by Aki (1967) predicts that the use of surface wave spectral amplitudes at 100-s period will severely underestimate (by a factor of 10–100) the seismic moment M_0 of any very large earthquake ($M \geqslant 8{\cdot}0$). If this ω^2 scaling law proposed by Aki (1967) is valid for these very large magnitude earthquakes, then the slip-areas associated with many past large magnitude earthquakes may have been severely underestimated. Brune & King (1967) present evidence which casts some doubt on the validity of the ω^2 model of Aki (1967) for the very large magnitude ($M \geqslant 8{\cdot}0$) earthquakes, but in any case it seems fairly clear that the slip-area vs. magnitude relation in equation (55) will be increasingly inaccurate for larger magnitude earthquakes. For example, it can be seen from Fig. 9 that the relation (55) underestimates all the moments determined by Kanamori (1970) from analysis of longer period (> 100 s) surface waves. It is likely then that the slip-areas $[A_0\,\overline{\Delta v}_0]$ of the very largest earthquakes have been systematically underestimated by using the relation (55). Since it is the few largest earthquakes which dominate the contribution to the random walk process used to estimate $\langle R^2 \rangle$, this quantity may have been significantly underestimated through the use of (55).

There is thus some evidence then that the seismic slip-areas of at least the very largest earthquakes may have been underestimated because the use of a moment–magnitude relation based on the excitation of 100-s surface waves is inadequate. There is also reason to believe that the slip-areas of all shallow focus thrust fault type earthquakes have been systematically underestimated.

About 70 per cent of past large earthquakes were shallow focus earthquakes located either in ocean trench or island arc zones or in continental compressive zones, and thus were presumably associated with a shallow angle thrust faulting mechanism. Davies & Brune (1971) have pointed out that for earthquakes associated with thrust faulting on fault plane dipping at angles less than about 30°, the slip-area inferred from (55) will be systematically underestimated. This is so because the efficiency of surface wave generation by a shallow focus dip slip earthquake falls off as sin 2δ where δ is the dip of the associated fault plant (Ben-Menahem & Harkrider 1954). Mitronovas, Isacks & Seeber (1969) have shown that carefully located earthquake hypocentres can be used to accurately define the location of the inclined zone of shallower depths in the lithosphere (depths h less than about 50 km) the seismic zone appears to decrease in dip or bend over sharply. This suggests strongly that shallow focus earthquakes occurring in the Tonga island arc region are associated for the most part with fault plane dip angles δ significantly less than 45°. Both focal mechanism studies (Stauder & Bollinger 1966) and field evidence (Plafker 1969) indicate that the fault plane associated with the 1964 Alaskan earthquake dips at an extremely shallow angle, 5° to 15°. Malahoff (1970) has suggested a mechanism whereby the near-vertical gravity faulting observed in marine refraction profiles of sediment-filled oceanic trenches can be reconciled with shallow dip (δ about 20°) thrust faulting in the lithosphere behind the oceanic trenches. Evidence of this kind makes it appear very likely that most thrust faulting at shallow depths in island arc and oceanic trench areas is associated with dip angles δ of 30° or less. If this is true, then use of the relation (55) will result in a systematic underestimate of the slip-area $[A_0\,\Delta v_0]$ for up to 70 per cent of the Earth's past earthquakes. Davies & Brune (1971) were fully aware of this when they used the moment–magnitude relation to compute fault slip rates from seismicity. In fact they point out how this effect will tend to be cancelled out by another assumption which they make in the calculation of fault slippage rates on shallow angle thrust faults with dip less than 30°. The systematic underestimate of earthquake slip-areas $[A_0\,\overline{\Delta v}_0]$ associated with oceanic trench area thrust faults of shallow dip will of course result in an even greater underestimate of $\langle R^2\rangle$; the magnitude of this effect is uncertain.

The fact that many large earthquakes have an associated sequence of smaller aftershocks is another reason why $\langle R^2\rangle$ has probably been underestimated. It is true that in general smaller magnitude earthquakes contribute very little to the net pole shift per year $\langle R^2\rangle$. This is due to the fact that the slip-area of an individual earthquake is logarithmically related to the magnitude M as well as to the fact that smaller step sizes contribute little toward the final outcome of a random walk process. If however a smaller earthquake is an aftershock of a large earthquake, then the situation is different. Stauder & Bollinger (1966) and Stauder (1968), using first motion focal mechanism studies, have shown that the aftershock sequences of both the 1964 Alaskan earthquake and the 1965 Rat Island earthquake had a common faulting mechanism which was in both cases the same as that of the associated main shock. It is probably generally true that aftershocks associated with any large shallow focus earthquake located on a major plate boundary will have the same faulting mechanism as the main shock. If that is the case, then any aftershock occurring fairly soon (compared to 14 months) after a large main shock will have the effect of increasing the net effective slip-area $[A_0\,\overline{\Delta v}_0]$ of that shock. In other words, for the purpose of estimating $\langle R^2\rangle$, one should consider the slip-areas $[A_0\,\overline{\Delta v}_0]$ of individual large shallow focus earthquakes to be the slip-area of the main shock augmented by the net slip-area release of the first few weeks of aftershock activity. It appears that no one has ever made a study of the slip-area release (or moment accumulation) of the earthquakes in an aftershock sequence (Brune, personal communication). Båth & Benioff (1958) have however made a study of what they have called the strain release associated with the aftershock sequence of the 1952 November 4 Kamchatka earth-

quake ($M = 8{\cdot}4$, $M_m = 8{\cdot}8$). The strain release $J^{\frac{1}{2}}$ associated with an earthquake of magnitude M is defined by Båth & Benioff (1958) as

$$\log_{10} J^{\frac{1}{2}} = 4{\cdot}5 + 0{\cdot}9\, M. \tag{57}$$

Their plot of aftershock strain release—versus time after the main shock indicates that the first two to three weeks of aftershock activity accounted for almost twice as much strain release as the initial main shock. On the other hand, Duda (1963) has performed a similar strain release study on the 1960 Chilean earthquake and found that the aftershock sequence was relatively unimportant in relation to the main shock. It is difficult to convert directly data on aftershock strain release into data on aftershock slip-area release. It seems likely however, from the work of Båth & Benioff (1958), that the aftershock sequences associated with at least some large earthquakes may significantly increase the effective earthquake slip-area, by as much as 50–100 per cent.

Another observed phenomenon which could be very important in any attempted estimation of seismically generated Chandler wobble activity is earthquake-generated or earthquake-associated fault creep. Aseismic fault creep sequences have been observed to occur on the San Andreas fault in conjunction with and seemingly directly produced by intermediate magnitude earthquakes (Scholz, Wyss & Smith 1969). The best studied creep sequence is that following the Parkfield earthquake ($M = 5{\cdot}5$) which occurred on the San Andreas fault on 1966 June 27. After the main Parkfield shock, slow slippage of the San Andreas fault in the epicentral area began to occur and continued to occur thereafter, the slippage rate decaying approximately logarithmically in time. Scholz *et al.* (1969) have interpreted fault creep sequences following earthquakes as a slippage occurring on portions of the fault surface which did not slip at the time of the main shock. They suggest, for example, that the main Parkfield earthquake occurred at a depth greater than 4 km and that then the stress across the fault above 4 km depth was achieved by a slow aseismic slippage. These observations of aseismic fault slippage following earthquakes are very pertinent to any study of the excitation of the Chandler wobble by earthquakes. Any fault creep which occurs in the first few weeks (a time period short compared to 14 months) after a particular earthquake will have the effect of raising the effective slip area of that earthquake. Thus the earthquake slip-area which is effective in exciting the Chandler wobble is the slip-area of the main shock augmented not only by the net slip-area release of the first few weeks of aftershock activity but also by the net slip area release of the first few weeks of associated aseismic creep. Because of the possibility of aseismic fault creep associated with earthquakes, any seismic measure of earthquake slip-areas may severely underestimate the effective slip-areas which should be used in estimating $\langle R^2 \rangle$. For this reason, even a large scale project like that proposed by Brune & Jarosch (personal communication) to measure the long period surface wave seismic moments M_0 of all past large earthquakes may not provide sufficient information about effective earthquake slip-areas to allow a conclusive test of the hypothesis that earthquakes maintain the Chandler wobble. Observations of aseismic fault creep following earthquakes are very recent and it is not at all clear how large an effect this might have on estimation of $\langle R^2 \rangle$ It does certainly not seem unreasonable that the Chandler wobble effective slip-areas of many large earthquakes could be 5–10 times greater than the seismic slip-areas deduced from a study of the seismic waves and free oscillations excited by the main shock because of this effect.

One further related possibility should perhaps be mentioned It is clear that any process in the Earth which results in a redistribution in the Earth's mass in a time period short compared to 14 months will act to excite the Chandler wobble. It is also clear that any aseismic slippage on a fault surface (not necessarily following an

earthquake) which occurs in a time period short compared to 14 months will produce a net elastic gravitational for field strain exactly the same as if the slippage had occurred instantaneously. It is certainly conceivable that there may be slippage on many faults or other surfaces within the Earth which occurs aseismically but with a time scale which is short compared to 14 months. For example, the downward motion of lithospheric plates in the deep Benioff zones behind island arcs may be occurring in this way. This deep slippage does appear to be occurring almost aseismically (Brune 1968; Isacks *et al.* 1968), but it may be that it would appear episodic on a 14 month time scale. Virtually nothing is known about the nature of the slippage in these deep zones and it may turn out that some such unknown phenomenon plays a crucial role in maintaining the observed activity of the Chandler wobble.

In view of the large uncertainties in the estimation of the slip-areas associated with past earthquakes and especially in view of the several reasons why many of the slip-areas may have been underestimated in this study, it seems reasonable to say that the agreement between the computed and observed Chandler wobble power P is about as good as could be expected. Present information about the slip-areas of past earthquakes and about the possibility of aseismic fault slippage following earthquakes is insufficient to allow a really conclusive test of the hypothesis that earthquakes maintain the Earth's Chandler wobble.

6. Conclusions

In this paper an attempt has been made to test the hypothesis that earthquakes are responsible for the generation and maintenance of the Earth's Chandler wobble. It was shown how elastic dislocation theory could be extended in order to compute the changes in the inertia tensor produced by an arbitrary point tangential displacement dislocation in an arbitrary spherically symmetric, non-rotating, perfectly elastic, isotropic (SNREI) Earth model. This theory can be used to deduce the effect on the Earth's instantaneous pole of rotation of any past earthquake for which the location, size, and geometry of the associated faulting can be specified. Numerical computations have been performed using a particular self-gravitating SNREI Earth model which has a fluid core, and which has realistic radial variations in density and in the elastic velocities. The magnitude and direction of the shifts of the mean pole of rotation produced by both the 1960 Chilean earthquake and the 1964 Alaskan earthquake were computed and compared with the polar shifts inferred from the astronomical data by Smylie & Mansinha (1968). The theory was also used to estimate the total Chandler wobble power which would have been produced by all large earthquakes ($M \leqslant 7{\cdot}0$) which occurred in the 60-year span 1904–1964, and this was compared with the Earth's total observed Chandler wobble power. An empirical earthquake moment–magnitude relation of Brune (1968) was used to infer the slip-areas associated with past large earthquakes.

The principal results and conclusions of this work are summarized here.

1. The computed polar shifts produced by the 1960 Chilean and 1964 Alaskan earthquakes showed a complete lack of agreement with the polar shifts inferred from the astronomical data by Smylie & Mansinha (1968). It was pointed out that the polar motion data analysis procedure used by Smylie & Mansinha (1968) may be invalidated by their neglect of the slow motion of the mean rotation pole between the times of occurrence of earthquakes. If noise contamination of the astronomical data is not too severe, then a re-analysis of the data may produce results which accord better with the theoretical results presented here.

2. Changes in the Earth's inertia tensor produced by large earthquakes are sufficiently large that it is extremely plausible that seismic activity is sufficient to maintain the Earth's Chandler wobble. Depending on the Q of the Chandler wobble, all that is required to maintain the observed level of Chandler wobble activity is one earthquake the size of the 1964 Alaskan earthquake every 1–3 years. A more definitive conclusion about Chandler wobble maintenance by earthquakes is precluded because of a lack of sufficient information about the slip-areas associated with past large earthquakes. It is likely that even a more accurate determination of the seismic moments of past large earthquakes will not provide sufficient information to make a definitive conclusion, because of the largely unknown effects of aftershock sequences and aseismic fault creep.

3. New observational techniques (e.g. the lunar laser reflector) may someday provide much more accurate determinations of the actual motion of the Earth's instantaneous pole of rotation. In that case, the theory presented here may be used not only to determine seismic focal mechanisms and seismic slip-areas associated with future earthquakes, but also perhaps to infer information about the time behaviour of aseismic fault creep and elastic strain build-up within the Earth.

Acknowledgments

Most of this work was done while I was an NSF postdoctoral fellow at the Department of Geodesy and Geophysics, Cambridge University, Cambridge, England, and I am grateful to Sir Edward Bullard and other members of the department for making my stay there so pleasant. I have benefited from either conversation or correspondence with K. Aki, Jim Brune, Geoffreys Davies, Peter Fellgett, Dick Haubrich, Sir Harold Jeffreys, Dan McKenzie and H. Kanamori.

Department of Geological and Geophysical Sciences,
Princeton University,
Princeton,
New Jersey

References

Aki, K., 1966. Generation and propagation of G waves from Niigata earthquake of June 16, 1964, *Bull. Earthquake Res. Inst. Tokyo Univ.*, **44,** 73–88.

Aki, K., 1967. Scaling law of seismic spectrum, *J. geophys. Res.*, **72,** 1217–1231.

Alterman, Z., Jarosch, H. & Pekeris, C. L., 1959. Oscillations of the Earth, *Proc. R. Soc.*, **A252,** 80–95.

Backus, G. E., 1967. Converting vector and tensor equations to scalar equations in spherical co-ordinates, *Geophys. J. R. astr. Soc.*, **13,** 71–101.

Backus, G. E. & Gilbert, F., 1967. Numerical applications of a formalism for geophysical inverse problems, *Geophys. J. R. astr. Soc.*, **13,** 247–276.

Båth, M. & Benioff, H., 1958. The aftershock sequence of the Kamchatka earthquake of November 4, 1952, *Bull. seism. Soc. Am.*, **48,** 1–15.

Ben-Menahem, A. & Harkrider, D., 1964. Radiation patterns of seismic surface waves from buried dipolar point sources in a flat stratified Earth, *J. geophys. Res.*, **69,** 2605–2620.

Ben-Menahem, A. & Israel, M., 1970. Effects of major seismic events on the rotation of the Earth, *Geophys. J. R. astr. Soc.*, **19,** 367–393.

Ben-Menahem, A. & Singh, S. J., 1968. Eigenvector expansions of Green's dyads with applications to geophysical theory, *Geophys. J. R. astr. Soc.*, **16,** 417–452.

Brune, J. N., 1968. Seismic moment, seismicity, and rate of slip along major fault zones, *J. geophys. Res.*, **73,** 777–784.

Brune, J. N. & Allen, C. R., 1961. A low stress-drop, low magnitude earthquake with surface faulting: the Imperial, California of March 4, 1966. *Bull. seism. Soc. Am.*, **57,** 501–514.

Brune, J. N. & Engen, G. R., 1969. Excitation of mantle Love waves and definition of mantle wave magnitude, *Bull. seism. Soc. Am.*, **59,** 923–933.

Brune, J. N. & King, C. Y., 1967. Excitation of mantle Rayleigh waves of period 100 seconds as a function of magnitude, *Bull. seism. Soc. Am.*, **59,** 1355–1365.

Burridge, R. & Knopoff, L., 1964. Body force equivalents for seismic dislocations, *Bull. seism. Soc. Am.*, **54,** 1875–1888.

Cecchini, G., 1928. Il problema della variazione delle latitudini, *Publ. Reale Obs. Astr. Brera in Milano*, **61,** 7–96.

Chinnery, M. A., 1961. The deformation of the ground around surface faults, *Bull. seism. Soc. Am.*, **51,** 355–372.

Dahlen, F. A., 1968. The normal modes of a rotating, elliptical Earth, *Geophys. J. R. astr. Soc.*, **16,** 329–367.

Davies, G. F. & Brune, J. N., 1971. Regional and global fault slip rates from seismicity, *Nature*, in press.

Duda, S. J., 1963. Strain release in the Circum-Pacific belt, Chile: 1960, *J. geophys. Res.*, **68,** 5531–5544.

Duda, S. J., 1965. Secular seismic energy release in the Circum-Pacific belt, *Tectonophysics*, **2,** 409–452.

Goldreich, P. & Toomre, A., 1969. Some remarks on polar wandering, *J. geophys. Res.*, **74,** 2555–2567.

Gutenberg, B. & Richter, C. F., 1954. *Seismicity of the Earth and associated phenomena*, Princeton University Press, 310 pp.

Haubrich, R., 1970. An examination of the data relating pole motion to earthquakes, *Earthquake displacement fields and the rotation of the Earth*, ed. by Mansinha, L., *et al.*, D. Reidel, Dordrecht.

Haubrich, R. & Munk, W., 1959. The pole tide, *J. geophys. Res.*, **64,** 2373–2388.

Hide, R., 1969. Interaction between the Earth's liquid core and solid mantle, *Nature*, **222,** 1055–1056.

Hodgson, J. H., 1957. Nature of faulting in large earthquakes, *Geol. Soc. Am. Bull.*, **68,** 611–644.

Isacks, B. J., Oliver, J. & Sykes, L. R., 1968. Seismology and the new global tectonics, *J. geophys. Res.*, **73,** 5855–5899.

Jeffreys, H., 1916. Causes contributory to the annual variation of latitude, *Mon. Not. R. astr. Soc.*, **76,** 499–525.

Jeffreys, H., 1940. The variation of latitude, *Mon. Not. R. astr. Soc.*, **100,** 139–155.

Jeffreys, H., 1963. The hydrostatic theory of the figure of the Earth, *Geophys. J. R. astr. Soc.*, **8,** 196–202.

Jeffreys, H., 1968. The variation of latitude, *Mon. Not. R. astr. Soc.*, **141,** 255–268.

Jeffreys, H. & Vicente, R., 1957a. The theory of nutation and the variation of latitude, *Mon. Not. R. astr. Soc.*, **117,** 142–161.

Jeffreys, H. & Vicente, R., 1957b. The theory of nutation and the variation of latitude: the Roche model core, *Mont. Not. R. astr. Soc.*, **117,** 162–173.

Kanamori, H., 1970a. Synthesis of long period surface waves and its application to earthquake source studies—Kurile Islands earthquake of October 13, 1963. *J. geophys. Res.*, **75,** 5011–5028.

Kanamori, H., 1970b. The Alaska earthquake of 1964:.radiation of long period surface waves and source mechanism, *J. geophys. Res*, **75,** 5029–5040.

Larmor, J., 1909. The relation of the Earth's free precessional nutation to its resistance against tidal deformation, *Proc. R. Soc.*, **A82,** 89–96.

Le Pichon, X., 1968. Sea floor spreading and continental drift, *J. geophys. Res.*, **73,** 3661–3697.

Longman, I. M., 1963. A Green's function for determining the deformation of the Earth under surface mass loads, 2. Computations and numerical results, *J. geophys. Res.*, **68,** 485–496.

Love, A. E. H., 1909. The yielding of the Earth to disturbing forces, *Proc. R. Soc.*, **A82,** 73–88.

Love, A. E. H., 1927. *A treatise on the mathematical theory of elasticity*, New York, Dover Publications, 643 pp.

MacDonald, G. J. F., 1966. The figure and long term mechanical properties of the Earth, *Advances in Earth Science*, pp. 192–245, ed. by P. M. Hurley, Massachusetts Institute of Technology Press, Cambridge, Mass.

Malahoff, A., 1970. Some possible mechanisms for gravity and thrust faults under oceanic trenches, *J. geophys. Res.*, **75,** 1992–2001.

Mansinha, L. & Smylie, D. E., 1967. Effect of earthquakes on the Chandler wobble and the secular polar shift, *J. geophys. Res.*, **72,** 4731–4743.

Mansinha, L., Smylie, D. E. & Beck, A. E. (eds), 1970. *Earthquake displacement fields and the rotation of the Earth*, D. Reidel, Dordrecht, in press.

Maruyama, T., 1963. On the force equivalents of dynamical elastic dislocations with reference to the earthquake mechanism, *Bull. earthqu. Res. Inst., Tokyo Univ.*, **41,** 467–486.

Maruyama, T., 1964. Statical elastic dislocations in an infinite and semi-infinite medium, *Bull. earthqu. Res. Inst., Tokyo Univ.*, **42,** 289–368.

McKenzie, D. P., 1969. Speculations on the consequences and causes of plate motions, *Geophys. J. R. astr. Soc.*, **18,** 1–32.

McKenzie, D. P. & Parker, R. L., 1967. The North Pacific: an example of tectonics on a sphere, *Nature*, **216,** 1276–1280.

Mitronovas, W., Isacks, B. & Seeber, L., 1969. Earthquake locations and seismic wave propagation in the upper 250 km of the Tonga island arc, *Bull. seism. Soc. Am.*, **59,** 1115–1135.

Morgan, W. J., 1968. Rises, trenches, great faults, and crustal blocks, *J. geophys. Res.*, **73,** 1959–1981.

Munk, W. & Hassan, E. S. M., 1961. Atmospheric excitation of the Earth's wobble, *Geophys. J. R. astr. Soc.*, **4,** 339–358.

Munk, W. & MacDonald, G., 1960. *The rotation of the Earth, a geophysical discussion*, Cambridge University Press, 323 pp.

Newcomb, S., 1892. On the dynamics of the Earth's rotation, with respect to the periodic variations of latitude, *Mon. Not. R. astr. Soc.*, **52,** 336–341.

Pekeris, C. L. & Jarosch, H., 1958. The free oscillations of the Earth, *Contributions in Geophysics*, Pergamon Press, New York, 244 pp.

Plafker, G., 1965. Tectonic deformation associated with the 1964 Alaskan earthquake, *Science*, **148,** 1675–1687.

Plafker, G., 1969. Tectonics of the March 27, 1964 Alaska earthquake, *Geol. Survey Prof.* Paper 543–I, 74 pp.

Plafker, G. & Savage, J. C., 1970. Mechanism of the Chilean earthquakes of May 21 and 22, 1960. *Geol. Soc. Am. Bull.*, **81,** 1001–1030.

Press, F., 1965. Displacements, strains, and tilts at teleseismic distances, *J. geophys. Res.*, **70,** 2395–2412.

Richter, C. F., 1958. *Elementary seismology*, W. H. Freeman, San Francisco, 768 pp.

Rochester, M. G. & Smylie, D. E., 1965. Geomagnetic core–mantle coupling and the Chandler wobble, *Geophys. J. R. astr. Soc.*, **10,** 289–315.

Rudnick, P., 1956. The spectrum of the variation in latitude, *Trans. Am. geophys. Un.*, **37**, 137–142.
Scholz, C. H., Wyss, M. & Smith, S., 1969. Seismic and aseismic slip on the San Andreas Fault, *J. geophys. Res.*, **74**, 2049–2069.
Singh, S. J. & Ben-Menahem, A., 1969. Deformation of a homogeneous, gravitating sphere by internal dislocations, *Pure appl. Geophys.*, **76**, 17–39.
Slichter, L. B., 1967. Free oscillations of the Earth, *International Dictionary of Geophysics*, ed. by S. K. Runcorn, Pergamon Press Ltd, Oxford, pp. 331–343.
Smylie, D. E. & Mansinha, L., 1968. Earthquakes and the observed motion of the rotation pole, *J. geophys. Res.*, **73**, 7661–7673.
Stacey, F. D., 1969. *Physics of the Earth*, John Wiley and Sons, Inc., New York, 324 pp.
Stauder, W., 1968. Mechanism of the Rat Island earthquake sequence of February 4, 1965, with relation to island arcs and sea-floor spreading, *J. geophys. Res.*, **73**, 3847–3858.
Stauder, W. & Bollinger, G. A., 1966. The focal mechanism of the Alaska earthquake of March 28, 1964, and of its aftershock sequence, *J. geophys. Res.*, **71**, 5283–5296.
Steketee, J. A., 1958. On Volterra's dislocations in a semi-infinite elastic medium, *Can. J. Phys.*, **36**, 192–205.
Sykes, L. R., 1967. Mechanism of earthquakes and nature of faulting on the mid-oceanic ridges, *J. geophys. Res.*, **72**, 2131–2153.
Volterra, V., 1907. Sur l'équilibre des corps elastiques multipliquement connexes, *Paris, Ann. Ec. norm.* (Sér 3), **24**, 401–517.
Walker, A. & Young, A., 1957. Further results on the analysis of the variation of latitude, *Mon. Not. R. astr. Soc.*, **117**, 119–141.
Wyss, M. & Brune, J. N., 1968. Seismic moment, stress, and source dimensions for earthquakes in the California–Nevada region, *J. geophys. Res.*, **73**, 4681–4694.

Note Added in Proof

I have recently discovered that the argument leading to the Volterra relation for a tangential displacement dislocation equation (34) is incorrect in certain non-trivial details. The equation itself and its infinitesimal form equation (37) are however correct for a SNREI Earth model (except for the $l = 1$ harmonic term which must be treated separately as noted in Appendix A), and all the results and conclusions of the paper are unaffected. The necessary modifications to the argument are sufficiently interesting that they will be published sometime in the future.

Appendix A

Evaluation of ΔC_{13} and ΔC_{23}

Equation (48) shows how ΔC_{13} and ΔC_{23} may be computed in terms of four scalar radial functions $\mathscr{U}_2^1(r)$, $\tilde{\mathscr{U}}_2^1(r)$, $\mathscr{V}_2^1(r)$, $\tilde{\mathscr{V}}_2^1(r)$. The algebraic details necessary for the evaluation of $\mathscr{U}_2^1(r)$, $\tilde{\mathscr{U}}_2^1(r)$, $\mathscr{V}_2^1(r)$, $\tilde{\mathscr{V}}_2^1(r)$ are given here. These four functions $\mathscr{U}_2^1(r)$, $\tilde{\mathscr{U}}_2^1(r)$, $\mathscr{V}_2^1(r)$, $\tilde{\mathscr{V}}_2^1(r)$ are four of the radial coefficients in the vector spherical harmonic expansion (equations (38) and (42)) of the vector displacement field $\mathbf{v}(\mathbf{r})$ which is given by equation (37).

$$v_k(\mathbf{r}) = \hat{\mathbf{x}}_k \cdot \mathbf{v}(\mathbf{r}) = [A_0\, \overline{\Delta v_0}]\, tr\, [\hat{\mathbf{n}}_0\, \hat{\mathbf{e}}_0 \cdot \mathbf{E}^k(\mathbf{r}, \mathbf{r}_0)]. \tag{58}$$

The evaluation of equation (58) in terms of quantities suitable for numerical computation was considerably simplified by making use of the tangent tensor representation theorem and many consequent formulae of Backus (1967). No attempt has been made to make the exposition in this appendix self-contained; the content and notation of Backus (1967) are relied upon heavily.

Recall that $\mathbf{E}^k(\mathbf{r}, \mathbf{r}_0)$ in equation (58) is defined as the stress $\mathbf{E}$ produced at the point $\mathbf{r}_0$ (the location of the point tangential displacement dislocation) by a unit point force $\mathbf{f}(\mathbf{r}, \mathbf{r}')$ located at the point $\mathbf{r}$ and pointing in the direction $\mathbf{x}_k$. The point force $\mathbf{f}$ may be written as

$$\mathbf{f}(\mathbf{r}, \mathbf{r}') = \hat{\mathbf{x}}_k \delta(\mathbf{r}' - \mathbf{r})(r'^2 \sin\theta')^{-1} \tag{59}$$

where

$$\delta(\mathbf{r}' - \mathbf{r}) = \delta(r' - r)\,\delta(\theta' - \theta)\,\delta(\phi' - \phi). \tag{60}$$

Then

$$\int_V \mathbf{f}(\mathbf{r}, \mathbf{r}')\, dV' = \hat{\mathbf{x}}_k. \tag{61}$$

This is the sense in which $\mathbf{f}(\mathbf{r}, \mathbf{r}')$ may be said to be a unit point force. In order to evaluate the response of an arbitrary SNREI Earth model to such a unit point force $\mathbf{f}(\mathbf{r}, \mathbf{r}')$, it is convenient to utilize a vector spherical harmonic expansion of $\mathbf{f}(\mathbf{r}, \mathbf{r}')$

$$\mathbf{f}(\mathbf{r}, \mathbf{r}') = \hat{\mathbf{r}}'\, A(\mathbf{r}, \mathbf{r}') + \nabla_1'\, B(\mathbf{r}, \mathbf{r}') - \hat{\mathbf{r}}' \times \nabla_1'\, C(\mathbf{r}, \mathbf{r}') \tag{62}$$

where

$$\left.\begin{aligned} A(\mathbf{r}, \mathbf{r}') &= \sum_{l=0}^{\infty} \sum_{m=-l}^{l} \alpha_l^m(r, r')\, \overset{*}{Y}{}_l^m(\theta', \phi') \\ B(\mathbf{r}, \mathbf{r}') &= \sum_{l=0}^{\infty} \sum_{m=-l}^{l} \beta_l^m(r, r')\, \overset{*}{Y}{}_l^m(\theta', \phi') \\ C(\mathbf{r}, \mathbf{r}') &= \sum_{l=0}^{\infty} \sum_{m=-l}^{l} \gamma_l^m(r, r')\, \overset{*}{Y}{}_l^m(\theta', \phi'). \end{aligned}\right\} \tag{63}$$

The complex conjugate $\overset{*}{Y}{}_l^m(\theta', \phi')$ has been used in the expansion for convenience later on. It is easily shown that

$$\left.\begin{aligned} \alpha_l^m &= \hat{\mathbf{x}}_k \cdot \hat{\mathbf{r}}\, Y_l^m(\theta, \phi)\, \delta(r' - r)(r')^{-2} \\ l(l+1)\,\beta_l^m &= \hat{\mathbf{x}}_k \cdot \nabla_1\, Y_l^m(\theta, \phi)\, \delta(r' - r)(r')^{-2} \\ l(l+1)\,\gamma_l^m &= \hat{\mathbf{x}}_k \cdot [-\hat{\mathbf{r}} \times \nabla_1\, Y_l^m(\theta, \phi)]\, \delta(r' - r)(r')^{-2} \end{aligned}\right\} \tag{64}$$

The application of the unit point force $\mathbf{f}(\mathbf{r}, \mathbf{r}')$ causes a displacement field $\mathbf{S}^k(\mathbf{r}, \mathbf{r}')$ at all points $\mathbf{r}'$ in the Earth model V. This vector displacement field $\mathbf{S}^k(\mathbf{r}, \mathbf{r}')$ may also be represented by a vector spherical harmonic expansion.

$$S^k(\mathbf{r}, \mathbf{r}') = \hat{\mathbf{r}}'\, U^k(\mathbf{r}, \mathbf{r}') + \nabla_1\, V^k(\mathbf{r}, \mathbf{r}') - \hat{\mathbf{r}} \times \nabla_1\, W^k(\mathbf{r}, \mathbf{r}') \tag{65}$$

where

$$\left.\begin{aligned} U^k(\mathbf{r}, \mathbf{r}') &= \sum_{l=0}^{\infty} \sum_{m=-l}^{l} U_l^m(r, r')\, \overset{*}{Y}{}_l^m(\theta', \phi') \\ V^k(\mathbf{r}, \mathbf{r}') &= \sum_{l=0}^{\infty} \sum_{m=-l}^{l} V_l^m(r, r')\, \overset{*}{Y}{}_l^m(\theta', \phi') \\ W^k(\mathbf{r}, \mathbf{r}') &= \sum_{l=0}^{\infty} \sum_{m=-l}^{l} W_l^m(r, r')\, \overset{*}{Y}{}_l^m(\theta', \phi'). \end{aligned}\right\} \tag{66}$$

The equation relating $\mathbf{S}^k(\mathbf{r}, \mathbf{r}')$ to $\mathbf{f}(\mathbf{r}, \mathbf{r}')$ is equation (17) which is rewritten here

$$\left.\begin{aligned} -\rho\, \nabla' \phi_1 + \nabla' \cdot (\rho_0\, \mathbf{S})\, \nabla' \phi_0 - \nabla'(S \cdot \rho_0\, \nabla' \phi_0) + \nabla' \cdot \mathbf{E} + \mathbf{f} &= 0 \\ \nabla'^2 \phi_1 &= -4\pi G \nabla' \cdot (\rho_0\, \mathbf{S}) \end{aligned}\right\} \tag{67}$$

where $\mathbf{S}$ stands for $\mathbf{S}^k(\mathbf{r}, \mathbf{r}')$, $\mathbf{f}$ stands for $\mathbf{f}(\mathbf{r}, \mathbf{r}')$ and $\mathbf{E}$ stands for $\mathbf{E}^k(\mathbf{r}, \mathbf{r}')$. The equations (67) can be converted into first order coupled ordinary differential equations involving the scalar radial functions $U_l^m(r, r')$, $V_l^m(r, r')$, $W_l^m(r, r')$, etc. (Backus 1967). Since the toroidal part of the displacement field does not contribute to changes in the inertia tensor, only the poloidal system of equations will be considered. The poloidal system is of sixth order, there being six unknown gravitational-elastic quantities

$$U_l^m, V_l^m, P_l^m, Q_l^m, (\phi_1)_l^m, (g_1)_l^m$$

(Backus 1967). For convenience in what follows denote the homogeneous system of equations (Backus 1967, equations (5.35), (5.36), (5.37))

$$\left.\begin{aligned}
\partial_r U &= -\lambda(r\beta)^{-1}\,[2U - l(l+1)\,V] + \beta^{-1}\,P \\
\partial_r V &= r^{-1}[V - \mathcal{Q}^0\,U] + \mu^{-1}\,Q \\
r\partial_r P &= (4r^{-1}\,\gamma - 4\rho_0\,g_0)\,U - l(l+1)(2r^{-1}\,\gamma - \rho_0\,g_0)\,V \\
&\qquad + 2(\lambda\beta^{-1} - 1)\,P + l(l+1)\,Q + r\rho_0\,g_1 \\
r\partial_r Q &= \rho_0\,g_0 - 2r^{-1}\,\gamma)\,\mathcal{Q}_0\,U - r^{-1}[2\mu - l(l+1)(\gamma+\mu)]\,V \\
&\qquad - \lambda\beta^{-1}\,\mathcal{Q}_0\,P - 3Q + \rho_0\,\mathcal{Q}_0\,\phi_1 \\
\partial_r \phi_1 &= g_1 - 4\pi G\rho_0\,U \\
\partial_r g_1 &= -2r^{-1}\,g_1 + l(l+1)\,r^{-2}\,\phi_1 + 4\pi G\rho_0\,l(l+1)\,r^{-1}\,V
\end{aligned}\right\} \tag{68}$$

by the shorthand notation

$$\partial_r \Phi(r) = A(r)\,\Phi(r) \tag{69}$$

where

$$\Phi = \begin{bmatrix} U \\ V \\ P \\ Q \\ \phi_1 \\ g_1 \end{bmatrix}. \tag{70}$$

In equation (68)

$$\lambda = \kappa - \tfrac{2}{3}\mu,\ \beta = \lambda + 2\mu,\ \gamma = \lambda + \mu - \lambda^2\,\beta^{-1}.$$

In terms of this notation, the non-homogeneous equation (67) can be reduced to the non-homogeneous poloidal system

$$\partial_{r'}\,\Phi(r, r') = A(r')\,\Phi(r, r') - \alpha_l^m(r, r')\,I_P - \beta_l^m(r, r')\,I_Q \tag{71}$$

where

$$I_P = \begin{bmatrix} 0 \\ 0 \\ 1 \\ 0 \\ 0 \\ 0 \end{bmatrix}, \qquad I_Q = \begin{bmatrix} 0 \\ 0 \\ 0 \\ 1 \\ 0 \\ 0 \end{bmatrix}.$$

If $\Phi(r, r')$ is evaluated at $r' = r_0$, then $\mathbf{S}^k(\mathbf{r}, \mathbf{r}_0)$ and $\mathbf{E}^k(\mathbf{r}, \mathbf{r}_0)$ are known. The system of equations (71) is most easily solved for $\Phi(r, r_0)$ by utilizing reciprocity. Let $U_l^P(r_0, r)$, $V_l^P(r_0, r)$, etc. be the solution satisfying the proper boundary conditions to the system

$$\partial_r\,\Phi^P(r_0, r) = A(r)\,\Phi^P(r_0, r) - \delta(r - r_0)(r_0^{-2})\,I_P, \tag{72}$$

and let $U_l^Q(r_0, r_0)$, $V_l^Q, (r_0, r)$, etc. be the solution satisfying the proper boundary conditions to the system

$$\partial_r\,\Phi^Q(r_0, r) = A(r)\,\Phi^Q(r_0, r) - \delta(r - r_0)(r_0^{-2})\,I_Q. \tag{73}$$

Since $\Phi_l^P(r_0, r) = \Phi_l^P(r, r_0)$ and $\Phi_l^Q(r_0, r) = \Phi_l^Q(r, r_0)$, one can write the solution to (71) in the form

$$\mathbf{S}^k(\mathbf{r}, \mathbf{r}_0) = \sum_{l=0}^{\infty} \sum_{m=-l}^{l} [U_l^m(r, r_0)\, \hat{\mathbf{r}}\, \overset{*}{Y}_l^m(\theta_0, \phi_0) + V_l^m(r, r_0)\, \nabla_1\, \overset{*}{Y}_l^m(\theta_0, \phi_0)] \tag{74}$$

where

$$\left.\begin{aligned} U_l^m(r, r_0) &= \hat{\mathbf{x}}_k \cdot [U_l^P(r_0, r)\, \hat{\mathbf{r}}\, Y_l^m(\theta, \phi) + V_l^P(r_0, r)\, \nabla_1\, Y_l^m(\theta, \phi)] \\ V_l^m(r, r_0) &= \hat{\mathbf{x}}_k \cdot [U_l^Q(r_0, r)\, \hat{\mathbf{r}}\, Y_l^m(\theta, \phi) + V_l^Q(r_0, r)\, \nabla_1\, Y_l^m(\theta, \phi)]. \end{aligned}\right\} \tag{75}$$

The scalar radial functions $U_l^P(r_0, r)$, $V_l^P(r_0, r)$, $U_l^Q(r_0, r)$, $V_l^Q(r_0, r)$ may be numerically computed for any arbitrary SNREI Earth model. A variable order Runge–Kutta integration scheme developed and programmed by F. Gilbert for use in free oscillation studies was used for this purpose. The stress $\mathbf{E}^k(\mathbf{r}, \mathbf{r}_0)$ may be obtained from $\mathbf{S}^k(\mathbf{r}, \mathbf{r}_0)$ by utilizing the scalar potential representation for $\mathbf{E}^k(\mathbf{r}, \mathbf{r}_P)$ and by making use of the equations (5.30) in Backus (1967). Thus the four scalar potentials which serve to define the poloidal field part of the symmetric stress tensor $\mathbf{E}^k(\mathbf{r}, \mathbf{r}_0)$ may be written as

$$\left.\begin{aligned} P_l^m(r, r_0) &= \beta(\partial_r U) + \lambda r^{-1}[2U - l(l+1)\, V] \\ Q_l^m(r, r_0) &= \mu[(r\partial_r - 1)\, V + \mathscr{Q}_0\, U] \\ L_l^m(r, r_0) &= \lambda(\partial_r U) + (\lambda + \mu)\, r^{-1}[2U - l(l+1)\, V] \\ M_l^m(r, r_0) &= \mu r^{-1}\, \mathscr{Q}_1\, V \end{aligned}\right\} \tag{76}$$

In (76), U stands for $U_l^m(r, r_0)$ and V stands for $V_l^m(r, r_0)$.

Consider now the evaluation of expression (58). Following Backus (1967), write

$$\left.\begin{aligned} \mathbf{E}^k &= \hat{\mathbf{r}}\hat{\mathbf{r}} P + \hat{\mathbf{r}}\mathbf{E}_{rS} + \mathbf{E}_{rS}\, \hat{\mathbf{r}} + \mathbf{E}_{SS} \\ \hat{\mathbf{n}}_0 &= \hat{\mathbf{r}} n_r + \hat{\mathbf{n}}_S \\ \hat{\mathbf{e}}_0 &= \hat{\mathbf{r}} e_r + \mathbf{e}_S \end{aligned}\right\} \tag{77}$$

Then

$$tr(\hat{\mathbf{n}}_0\, \hat{\mathbf{e}}_0 \cdot \mathbf{E}^k) = n_r\, e_r\, P + (e_r\, \mathbf{n}_S + n_r\, \mathbf{e}_S) \cdot \mathbf{E}_r^S + tr(\mathbf{n}_S\, \mathbf{e}_S \cdot \mathbf{E}_{SS}). \tag{78}$$

As an example, consider the first term in (78)

$$n_r\, e_r\, P = n_r\, e_r \sum_{l=0}^{\infty} \sum_{m=-l}^{l} P_l^m(r, r_0)\, \overset{*}{Y}_l^m(\theta_0, \phi_0) \tag{79}$$

where $P_l^m(r, r_0)$ is obtained from equations (75), or in fact since the equations (75) are included in the system of equations (71)

$$P_l^m(r, r_0) = \hat{\mathbf{x}}_k \cdot [P_l^P(r_0, r)\, \hat{\mathbf{r}}\, Y_l^m(\theta, \phi)] + \hat{\mathbf{x}}_k \cdot [P_l^Q(r_0, r)\, \nabla_1\, Y_l^m(\theta, \phi)]. \tag{80}$$

Thus

$$n_r\, e_r\, P = \hat{\mathbf{x}}_k \cdot \sum_{l=0}^{\infty} \sum_{m=-l}^{l} [P_l^P(r_0, r)\, \overset{*}{Y}_l^m(\theta_0, \phi_0)\, \hat{\mathbf{r}}\, Y_l^m(\theta, \phi) + P_l^Q(r_0, r)\, \overset{*}{Y}_l^m(\theta_0, \phi_0)\, \nabla_1\, Y_l^m(\theta, \phi)]. \tag{81}$$

The left-hand side of (81) is of the form

$$\hat{\mathbf{x}}_k \cdot \sum_{l=0}^{\infty} \sum_{m=-l}^{l} [\hat{\mathbf{r}}\mathscr{U}_l^m(r)\, Y_l^m(\theta, \phi) + \mathscr{V}_l^m(r)\, \nabla_1\, Y_l^m(\theta, \phi)] \tag{82}$$

where

$$\left.\begin{aligned}\mathscr{U}_l^m(r) &= P_l^P(r_0, r)\ \overset{*}{Y}_l^m(\theta_0, \phi_0) \\ \mathscr{V}_l^m(r) &= P_l^Q(r_0, r)\ \overset{*}{Y}_l^m(\theta_0, \phi_0).\end{aligned}\right\} \tag{83}$$

Recall that equation (58) is an expression defining $\hat{\mathbf{x}}_k \cdot \mathbf{v}(\mathbf{r})$, the $\hat{\mathbf{x}}_k$ component of $\mathbf{v}(\mathbf{r})$. Note that since $\hat{\mathbf{x}}_k$ may be chosen arbitrarily, the expression (82) is in fact just the poloidal vector spherical harmonic expansion of $\mathbf{v}(\mathbf{r})$; the term $\hat{\mathbf{x}}_k$ may be eliminated from both sides of equation (58).

The second term in equation (78) is also easily evaluated. Its poloidal part is of the same form (82) where

$$\left.\begin{aligned}\mathscr{U}_l^m(r) &= (e_r\,\mathbf{n}_S + n_r\,\mathbf{e}_S) \cdot Q_l^P(r_0, r)\,\nabla_1\ \overset{*}{Y}_l^m(\theta_0, \phi_0) \\ \mathscr{V}_l^m(r) &= (e_r\,\mathbf{n}_S + n_r\,\mathbf{e}_S) \cdot Q_l^Q(r_0, r)\,\nabla_1\ \overset{*}{Y}_l^m(\theta_0, \phi_0).\end{aligned}\right\} \tag{84}$$

Evaluation of the third term in (78) is considerably more difficult, but considerations similar to those which lead to equation (4.16) in Backus (1967) enable one to carry out the evaluation. The final result for the poloidal part may again be put in the form (82) where

$$\begin{aligned}\mathscr{U}_l^m(r) = {} & M_l^P(r_0, r)[(\mathbf{n}_S \cdot \mathbf{e}_S)\ \overset{*}{Y}_l^m(\theta_0, \phi_0)] \\ & + L_l^P(r_0, r)\Big[(\mathbf{n}_S \cdot \mathbf{e}_S)\,\nabla_1^2\ \overset{*}{Y}_l^m(\theta_0, \phi_0) \\ & - \mathbf{n}_S \cdot \Big(-\hat{\mathbf{r}} \times \nabla_1 \Big(\mathbf{n}_S \cdot \big(-\hat{\mathbf{r}} \times \nabla_1\ \overset{*}{Y}_l^m(\theta_0, \phi_0)\big)\Big)\Big) \\ & - \mathbf{e}_S \cdot \Big(-\hat{\mathbf{r}} \times \nabla_1 \Big(\mathbf{n}_S \cdot \big(-\hat{\mathbf{r}} \times \nabla_1\ \overset{*}{Y}_l^m(\theta_0, \phi_0)\big)\Big)\Big) \\ & - (\nabla_1 \cdot \mathbf{e}_S)(\mathbf{n}_S \cdot \nabla_1\ \overset{*}{Y}_l^m(\theta_0, \phi_0)) \\ & - (\nabla_1 \cdot \mathbf{n}_S)(\mathbf{e}_S \cdot \nabla_1\ \overset{*}{Y}_l^m(\theta_0, \phi_0))\Big]\end{aligned} \tag{85}$$

similarly

$$\begin{aligned}\mathscr{V}_l^m(r) = {} & M_l^Q(r_0, r)[(\mathbf{n}_S \cdot \mathbf{e}_S)\ Y_l^m(\theta_0, \phi_0)] \\ & + L_l^Q(r_0, r)\Big[(\mathbf{n}_S \cdot \mathbf{e}_S)\,\nabla_1^2\ \overset{*}{Y}_l^m(\theta_0, \phi_0) \\ & - \mathbf{n}_S \cdot \Big(-\hat{\mathbf{r}} \times \nabla_1 \Big(\mathbf{e}_S \cdot \big(-\hat{\mathbf{r}} \times \nabla_1\ \overset{*}{Y}_l^m(\theta_0, \phi_0)\big)\Big)\Big) \\ & - \mathbf{e}_S \cdot \Big(-\hat{\mathbf{r}} \times \nabla_1 \Big(\mathbf{n}_S \cdot \big(-\mathbf{r} \times \nabla_1\ \overset{*}{Y}_l^m(\theta_0, \phi_0)\big)\Big)\Big) \\ & - (\nabla_1 \cdot \mathbf{e}_S)\mathbf{n}_S \cdot \nabla_1\ \overset{*}{Y}_l^m(\theta_0, \phi_0)) - (\nabla_1 \cdot \mathbf{n}_S)(\mathbf{e}_S \cdot \nabla_1\ \overset{*}{Y}_l^m(\theta_0, \phi_0))\Big].\end{aligned}$$

In equation (85) $M_l^P(r_0, r)$ and $L_l^Q(r_0, r)$ are obtained from equations (78) by substituting $U_l^P(r_0, r)$ and $\mathscr{V}_l^P(r_0, r)$ for U and V, and similarly for $M_l^Q(r_0, r)$ and $L_l^Q(r_0, r)$. The toroidal part of $\mathbf{v}(\mathbf{r})$ has also been evaluated in this manner but the results have not been given here. It should also be pointed that the above analysis is not valid for the case $l = 1$. The case $l = 1$ constitutes a special case and must be treated separately, since for $l = 1$ there exists a valid solution satisfying the boundary conditions to the homogeneous set of equations (68) (the solution is of the form $U = V =$ constant, and represents a rigid body translation of the Earth model).

The expressions (83), (84) and (85) defining $\mathbf{v}(\mathbf{r})$ in (82) may be reduced algebraically and put in a slightly more tractable form.

$$
\begin{aligned}
\mathscr{U}_l^m(r) = {} & P(r_0, r)[n_r\, e_r\, \overset{*}{Y}{}_l^m(\theta_0, \phi_0)^P{}_l] \\
& + Q_l^P(r_0, r)\left[(n_r\, e_\theta + n_\theta\, e_r)\,\frac{\partial\, \overset{*}{Y}{}_l^m}{\partial\theta}\,(\theta_0, \phi_0)\right. \\
& \left. + (n_r\, e_\phi + n_\phi\, e_r)\,\frac{1}{\sin\theta_0}\,\frac{\partial\, \overset{*}{Y}{}_l^m}{\partial\phi}\,(\theta_0, \phi_0)\right] \\
& + L_l^P(r_0, r)[(n_\theta\, e_\theta + n_\phi\, e_\phi)\, \overset{*}{Y}{}_l^m(\theta_0, \phi_0)] \\
& + M_l^P(r_0, r)[(n_\theta\, e_\theta - n_\phi\, e_\phi)\, l(l+1)\, \overset{*}{Y}{}_l^m(\theta_0, \phi_0) \\
& + 2(n_\theta\, e_\theta - n_\phi\, e_\phi)\,\frac{\partial^2\, \overset{*}{Y}{}_l^m}{\partial\theta^2}\,(\theta_0, \phi_0) \\
& + 2(n_\theta\, e_\phi + n_\phi\, e_\theta)\,\frac{\partial}{\partial\theta}\left[\frac{1}{\sin\theta}\,\frac{\partial\, \overset{*}{Y}{}_l^m}{\partial\phi}\right](\theta_0, \phi_0)] \\
\mathscr{V}_l^m(r) = {} & P_l^Q(r_0, r)[n_r\, e_r\, \overset{*}{Y}{}_l^m(\theta_0, \phi_0)] \\
& + Q_l^Q(r_0, r)\left[(n_r\, e_\theta + n_\theta\, e_r)\,\frac{\partial\, \overset{*}{Y}{}_l^m}{\partial\theta}\,(\theta_0, \phi_0)\right. \\
& \left. + (n_r\, e_\phi + n_\phi\, e_r)\,\frac{1}{\sin\theta_0}\,\frac{\partial\, \overset{*}{Y}{}_l^m}{\partial\phi}\,(\theta_0, \phi_0)\right] \\
& + L_l^Q(r_0, r)[(n_\theta\, e_\theta + n_\phi\, e_\phi)\, \overset{*}{Y}{}_l^m(\theta_0, \phi_0)] \\
& + M_l^Q(r_0, r)[(n_\theta\, e_\theta - n_\phi\, e_\phi)\, l(l+1)\, \overset{*}{Y}{}_l^m(\theta_0\, \phi_0) \\
& + 2(n_\theta\, e_\theta - n_\phi\, e_\phi)\,\frac{\partial^2\, \overset{*}{Y}{}_l^m}{\partial\theta^2}\,(\theta_0, \phi_0) \\
& + 2(n_\theta\, e_\phi + n_\phi\, e_\theta)\,\frac{\partial}{\partial\theta}\left(\frac{1}{\sin\theta}\,\frac{\partial\, \overset{*}{Y}{}_l^m}{\partial\phi}\right)(\theta_0, \phi_0)\Big]\,.
\end{aligned}
\tag{86}
$$

Actually in Section 3, $\mathbf{v}(\mathbf{r})$ was expanded not in the form (82) but rather in terms of A_l^m and B_l^m where $Y_l^m = A_l^m + iB_l^m$. It is easy to show that to compute $\mathscr{U}_l^m(r)$, $\mathscr{V}_l^m(r)$, $\tilde{\mathscr{U}}_l^m(r)$, $\tilde{\mathscr{V}}_l^m(r)$ as defined in Section 3, equation (42), one merely uses A_l^m and B_l^m in place of $\overset{*}{Y}{}_l^m$ in equations (86).

To compute ΔC_{13} and ΔC_{23}, one needs only $\mathscr{U}_2{}^1(r)$, $\mathscr{V}_2{}^1(r)$ and $\tilde{\mathscr{U}}_2{}^1(r)$, $\tilde{\mathscr{V}}_2{}^1(r)$. In equations (49), n_r, n_θ, n_ϕ, e_r, e_θ, e_ϕ are defined. Writing out equations (86) explicitly for $\mathscr{U}_2{}^1(r)$, $\mathscr{V}_2{}^1(r)$, $\tilde{\mathscr{U}}_2{}^1(r)$, $\tilde{\mathscr{V}}_2{}^1(r)$, one has:

$$
\begin{aligned}
\sqrt{\left(\frac{8\pi}{15}\right)}\,\mathscr{U}_2{}^1(r) = {} & M_l^P(r_0\, r)[(\sin 2\alpha\, \sin\delta\, \cos\lambda + \tfrac{1}{2}\cos 2\alpha\, \sin 2\delta\, \sin\lambda) \\
& \times \sin 2\theta_0\, \cos\phi_0 - 2(\tfrac{1}{2}\sin\, 2\alpha\, \sin 2\delta\, \sin\lambda - \cos 2\alpha\, \sin\delta\, \cos\lambda) \\
& \times \sin\theta_0\, \sin\phi_0] \\
& \tfrac{1}{4}[P_l^P(r_0, r) - L_l^P(r_0, r)][-\sin 2\delta\, \sin\lambda\, \sin 2\theta_0\, \cos\phi_0] \\
& + Q_l^P(r_0, r)[(\sin\alpha\, \cos 2\delta\, \sin\lambda - \cos\alpha\, \cos\delta\, \cos\lambda)\, \cos 2\theta_0\, \cos\phi_0 \\
& + (\sin\alpha\, \cos\delta\, \cos\lambda + \cos\alpha\, \cos 2\delta\, \sin\lambda)\, \cos\theta_0\, \sin\phi_0]
\end{aligned}
\tag{87}
$$

$$
\begin{aligned}
\sqrt{\left(\frac{8\pi}{15}\right)}\,\mathscr{V}_2{}^1(r) &= M_l{}^Q(r_0,r)[(\sin 2\alpha \sin\delta\cos\lambda+\tfrac{1}{2}\cos 2\alpha \sin 2\delta \sin\lambda)\\
&\times \sin 2\theta_0 \cos\phi_0\\
&-2(\tfrac{1}{2}\sin 2\alpha \sin 2\delta \sin\lambda-\cos 2\alpha \sin\delta\cos\lambda)\sin\theta_0 \sin\phi_0]\\
&+\tfrac{1}{4}[P_l{}^Q(r_0,r)-L_l{}^Q(r_0,r)][-\sin 2\delta \sin\lambda \sin 2\theta_0 \cos\phi_0]\\
&+Q_l{}^Q(r_0,r)[(\sin\alpha\cos 2\delta \sin\lambda-\cos\alpha\cos\delta\cos\lambda)\cos 2\theta_0\cos\phi_0\\
&+(\sin\alpha\cos\delta\cos\lambda-\cos\alpha\cos 2\delta\sin\lambda)\cos\theta_0\sin\phi_0]\\
\sqrt{\left(\frac{8\pi}{15}\right)}\,\tilde{\mathscr{U}}_2{}^1(r) &= M_l{}^P(r_0,r)[(\sin 2\alpha \sin\delta\cos\lambda+\tfrac{1}{2}\cos 2\alpha \sin 2\delta \sin\lambda)\\
&\times \sin 2\theta_0 \sin\phi_0\\
&+2(\tfrac{1}{2}\sin 2\alpha \sin 2\delta \sin\lambda-\cos 2\alpha \sin\delta\cos\lambda)\sin\theta_0\cos\phi_0]\\
&\times\tfrac{1}{4}[P_l{}^P(r_0,r)-L_l{}^P(r_0,r)][-\sin 2\delta \sin\lambda \sin 2\theta_0 \sin\phi_0]\\
&+Q_l{}^P(r_0,r)[(\sin\alpha\cos 2\delta \sin\lambda-\cos\alpha\cos\delta\cos\lambda)\cos 2\theta_0\sin\phi_0\\
&-(\sin\alpha\cos\delta\cos\lambda+\cos\alpha\cos 2\delta\sin\lambda)\cos\theta_0\cos\phi_0]\\
\sqrt{\left(\frac{8\pi}{15}\right)}\,\tilde{\mathscr{V}}_2{}^1(r) &= M_l{}^P(r_0,r)[(\sin 2\alpha \sin\delta\cos\lambda+\tfrac{1}{2}\cos 2\alpha \sin 2\delta \sin\lambda)\\
&\times \sin 2\theta_0 \sin\phi_0\\
&+2(\tfrac{1}{2}\sin 2\alpha \sin 2\delta \sin\lambda-\cos 2\alpha \sin\delta\cos\lambda)\sin\theta_0\cos\phi_0]\\
&\tfrac{1}{4}[P_l{}^Q(r_0,r)-L_l{}^Q(r_0,r)][-\sin 2\delta \sin\lambda \sin 2\theta_0 \sin\phi_0]\\
&+Q_l{}^Q(r_0,r)[(\sin\alpha\cos 2\delta \sin\lambda-\cos\alpha\cos\delta\cos\lambda)\cos 2\theta_0\sin\phi_0\\
&-(\sin\alpha\cos\delta\cos\lambda+\cos\alpha\cos 2\delta\sin\lambda)\cos\theta_0\cos\phi_0]
\end{aligned}
\qquad (87)\ (\textit{cont.})
$$

It is clear from examination of expressions (87) that when the integration in equations (48) is carried out that the final result will be of the form (50). The actual expressions for $\Gamma_1(h)$, $\Gamma_2(h)$, $\Gamma_3(h)$ will not be written out in full.

Appendix B

The effect of a fluid core

For various reasons, the procedure described in Appendix A must be altered if the SNREI Earth model under consideration has a fluid core. In the absence of both inertia and viscosity, individual fluid particles in a fluid core encounter no resistance to tangential (non-radial) motion. For this reason, the displacement $\mathbf{v}(\mathbf{r})$ within the fluid core due to a displacement dislocation (or any other static force) located within the solid elastic mantle becomes indeterminate. It will be shown however that the change in density $\rho_1(\mathbf{r})$ within the fluid core produced by a point tangential displacement dislocation located within the solid elastic crust or mantle is not indeterminate, and that thus the contribution of the fluid core to ΔC_{13} and ΔC_{23} may be computed.

Two problems arise in the case of a SNREI Earth model with a fluid core. The first problem arises in the solution of the two non-homogeneous poloidal systems (72) and (73). Longman (1963) has shown that the equations (68) cannot be satisfied in

a fluid core unless the density structure $\rho_0(r)$ of the fluid is such that the Adams–Williamson criterion is everywhere satisfied.

$$\partial_r \rho_0 + \rho_0 g_0{}^2 \lambda^{-1} = 0$$

where

$$g_0 = \partial_r \phi_0. \tag{88}$$

For this reason, the SNREI Earth model used in this work was modified to have an Adams–Williamson core. This adjustment would not be necessary if the steady diurnal rotation $\mathbf{\Omega}$ of the Earth were not neglected in deriving (68). Longman (1963) has shown that if (88) is satisfied in the core, then (68) reduces to

$$\left.\begin{aligned} &\mathscr{Q}_0[\partial_r \rho_0 U + \rho_0 X - \rho_0{}^2 \lambda^{-1} \phi_1] = 0 \\ &\nabla^2 \phi_1 = 4\pi G \rho_1 = -4\pi G(\partial_r \rho_0 + \rho_0 X) \end{aligned}\right\} \tag{89}$$

where X is the dilatation. Thus for a SNREI Earth model with a fluid core the equations (72) and (73) are solved by using (89) in the core, and the usual six-by-six system throughout the rest of the Earth. The boundary conditions at the core–mantle boundary remain unchanged: U, V, P, Q, ϕ_1, g_1 are continuous, except U, V, P are indeterminate within the core ($Q = 0$ in the core and from (88) and (89) the buoyant force combination $\mathscr{Q}_0[\rho_0 g_0 U - P]$ can be determined. See Longman (1963) for details on the correct boundary conditions at the core–mantle boundary.

Following Longman (1963), there is thus no difficulty in computing $\mathscr{U}_l^m(r)$, $\mathscr{V}_l^m(r)$ in the mantle of any SNREI Earth model with an Adams–Williamson fluid core. The second problem which arises in this application is the evaluation of the density change $\rho_1(\mathbf{r})$ in the fluid core. The displacement $\mathscr{U}_l^m(r)$, $\mathscr{V}_l^m(r)$ in the core is indeterminate, but the corresponding term $\mathscr{D}_l^m(r)$ for the density change $\rho_1(\mathbf{r})$ may be determined from (89)

$$\mathscr{Q}_0[\rho_1 + \rho_0{}^2 \lambda^{-1} \phi_1] = 0. \tag{90}$$

Thus $\mathscr{D}_l^m(r)$ in the fluid core is obtained not from $\mathscr{U}_l^m(r)$, $\mathscr{V}_l^m(r)$ but rather from $(\phi_1)_l^m(r)$ through the use of (90):

$$\mathscr{D}_l^m(r) = -C\rho_0{}^2 \lambda^{-1} (\phi_1)_l^m \tag{91}$$

where $(\phi_1)_l^m$ is obtained by solving (89) and where C is a constant obtained by satisfying the boundary condition that the gravitational potential change produced by the dislocation must be continuous across the core–mantle boundary. Pekeris & Jarosch (1958) have shown how to compute the change in gravitational potential at a radius r in terms of the poloidal displacement $\mathscr{U}_l^m(r)$, $\mathscr{V}_l^m(r)$ at the radius r. Using their result, one can determine the constant C in equation (91) in terms of $\mathscr{U} = \mathscr{U}_l^m(r)$, $\mathscr{V} = \mathscr{V}_l^m(r)$ in the mantle. Let $r = c$ and $r = a$ denote respectively the core–mantle boundary and the surface of the Earth model, let $\rho_0(c^-)$ denote the density of the fluid core at $r = c$, let $\phi_1(c)$, $\phi_1'(c)$ denote the values of $(\phi_1)_l^m$, $(\partial_r \phi_1)_l^m$ at $r = c$ obtained by solving the equations (89) in the fluid core.
Then

$$C = -4\pi G \left[\frac{(1/c) B(c) + \rho_0(c^-) \mathscr{U}(c)}{\phi_1'(c) + (l+1/c)\phi_1(c)} \right] \tag{92}$$

where

$$B(c) = c^l \int_c^a \rho_0 r^{-l} [-(l+1)\mathscr{U} + l(l+1)\mathscr{V}]\, dr$$

Thus $\mathscr{D}_l^m(r)$ may be determined in an Adams–Williamson fluid core.